A Study on the Development of an Electrically Assisted Smart Walker

Yuto Mori

Graduate School of Information Science and Technology

Hokkaido University

January, 2025

Contents

List of Figures

List of Tables

Chapter 1

Introduction

1.1 Background

The aging population in Japan is rapidly increasing each year, leading to a variety of challenges that cannot be easily addressed through conventional medical and nursing care systems. Recent attention has focused on healthy life expectancy [1, 2], which is defined as the difference between average life expectancy and nursing care period, with increasing emphasis on improving quality of life (QOL) [3]. Maintaining and improving walking function is essential for enhancing QOL, as evidenced by the prevalence of movement disorders as a primary cause of nursing care needs [4]. A decline in walking ability often results in decreased daily activity, potentially leading to a negative cycle of inadequate exercise and muscle weakness.

The Japanese Long-term Care-needs Certification [5] classifies care requirements into seven levels, ranging from Support Required Level 1-2 to Long-term Care Required Level 1-5. This classification system accommodates various care needs, from individuals who can walk with minimal support, such as handrails, to those requiring wheelchair mobility. In order to reduce the number of individuals requiring long-term care and the intensity of their care needs, it is essential to consider the utilization of appropriate care equipment and methodologies for each category.

As the global population continues to age, the need for walking assistance technologies is becoming increasingly evident. Walking represents the most fundamental and essential mode of human transportation, closely tied to the overall quality of life [6]. However, an individual's capacity for ambulation can decline owing to aging, illness, or accidents [7, 8, 9]. According to the basic survey on the lives of the people conducted by the Ministry of Health, Labor and Welfare in 2016 [10], locomotor disorders (locomotive syndrome) are the leading cause of individuals requiring nursing care, accounting for 24.6% of cases. To assist individuals with movement disorders, walking aids, such as canes, walkers, and wheelchairs have been developed. The use of these aids not only supports individuals in walking but also reduces the burden on caregivers, aligning with major public health goal [11].

Recent technological advancements have resulted in the electrification and robotization of walking aids [12, 13]. Compared with other forms of ambulation assistance, walkers provide moderate activity for lower body muscles while ensuring a high level of safety. The development of smart walkers aims to address the limitations of conventional walkers and offer more effective walking support. In smart walker research, motor-assisted propulsion is a primary method used to reduce the user's walking load.

1.1.1 Walking Aid

Walking aids are welfare equipment designed to assist the elderly and individuals with limited physical abilities in walking. Various devices are available, with options tailored to the user's physical capabilities and intended use. The three principal categories of walking aids are canes, rollators, and walkers.

Canes provide stability during walking by increasing the surface area of support, reducing lateral body movement, and distributing body weight to alleviate strain on the knees and lower back. They are ideal for individuals who can stand but feel insecure when walking without assistance, or those with mild symptoms who can walk short distances with some support. However, using a cane requires cognitive effort as users must determine the optimal placement while walking. A study conducted by Chen et al. [14] compared the attention demands of stroke patients walking with and without canes. The findings revealed that walking with canes increased attention demands.

Rollators are devices designed to assist elderly individuals who are capable of walking independently. These devices can be propelled by the user, providing a level of stability and support. In addition to the aforementioned simple walking aids, some rollators are also designed with features, such as storage for personal items and a seat for resting, making them particularly useful for outdoor activities.

Walkers, on the other hand, are walking aids that provide partial support for the user's body weight. The design of walkers ensures that the user's center of gravity remains within the frame while walking, enhancing stability. For a more detailed overview of the different types and functions of walkers, please refer to Section 1.1.2.

Other walking aids include walkers with a lifting function that supports the user's body by attaching to the waist [15]. Choosing the right walking aid can be challenging, as each aid is suited for different environments and levels of care. Furthermore, the specific needs of the user should be considered when selecting a walking aid. This study focuses on walking in a nursing home with multiple rooms and common spaces. The target users are assumed to be light-duty care recipients who can walk with some support. The primary focus will be on walkers that offer high stability and support for walking.

1.1.2 Walker and Smart Walker

A walker is a mobility aid designed to support a portion of the user's body weight while walking. Walkers can be classified into the following main types.

1. Walking frame or pickup walker
2. Two-wheel walker
3. Three-wheel walker
4. Four-wheel walker
5. Forearm support walker or forearm walker

A walking frame is a type of walker without wheels and features non-slip rubber or other materials on the tips of the four legs. This design provides excellent stability as the main body of the walker remains stationary while walking. However, it requires sufficient upper-body strength to lift and move the walker. Additionally, the four legs must remain in contact with the ground, making it suitable for indoor use on flat surfaces.

A wheel walker, on the other hand, is equipped with wheels on its legs and is maneuvered by holding onto the grips at the top of the central unit. A two-wheel walker has wheels attached to the front legs and is preferred by individuals who struggle with lifting a walking frame. Three-wheel and four-wheel walkers have wheels on all four legs, allowing for free direction changes while supporting the user's weight.

Figure 1.1: Forearm support walker with adjustable height support platform and four-wheel base.

Four-wheel walkers have a lower risk of falls in the lateral direction compared with two-wheel walkers [16].

A forearm support walker is a mobility aid that allows users to distribute their weight on the walker using their forearms. It is known for its high weight-bearing capacity, providing users with stability and support. It is often equipped with four wheels. A typical forearm support walker is shown in Figure 1.1, which is widely available on the market.

Because each walker has its advantages and disadvantages, they should be selected based on the specific needs and physical abilities. In recent years, a surge in research on smart walkers, which are equipped with sensors and motors to enhance usability and mitigate the limitations of traditional walkers, has been observed. These innovative devices are also known as robot walkers or intelligent walkers; however, for the purpose of this study, we will refer to them as smart walkers. Initially designed in the 2000s [17, 18] as mobility aids for individuals with visual impairments and walking disabilities, smart walkers have evolved to cater to a broader range of users, including those with mild mobility issues.

1.2 Research Objective

The goal of this study is to facilitate the recovery of complete independence and prevent the progression to a state requiring extensive care for individuals who can walk independently but may benefit from partial weight support. In recent years, a notable increase in the number of individuals with mild walking disabilities who rely on walking aids for assistance has been observed. This trend is particularly evident in Japan's long-term care certification system, where the number of individuals classified as requiring Long-term Care Level 1 or less has been steadily rising. By providing individuals with mild walking disabilities with the opportunity to walk independently, caregivers can focus on dealing with people with severe walking disabilities.

This study proposes the development of an electrically assisted forearm support smart walker to assist individuals with mild walking disabilities. This walker aims to address the challenges associated with conventional walkers, allowing users to navigate independently in nursing homes with shared spaces and private rooms, where users can independently navigate to common areas and other locations using the walker, aiming to increase their physical activity levels.

In the identified environment, several key issues have been recognized. First, the high cost of providing walkers on a loan basis in nursing homes can hinder user independence. Users often need to rely on caregivers to access a walker, impacting their ability to move freely. Second, the weight of traditional walkers can require increased propulsion force, making walking more challenging for users. The larger walkers are designed to provide increased stability and weigh approximately 7 to 13 kg. Consequently, they require more effort to propel forward compared with regular walking. Third, another concern to consider is the potential risk of falling owing to collisions. Although walkers provide significant support for body weight, they can easily tip over if the user loses their balance. Collisions with walls or obstacles can also lead to sudden changes in speed, further increasing the likelihood of a fall. Given that falls among the elderly often result in broken bones and other serious injuries, enhancing safety measures is a critical priority.

To address these challenges comprehensively, this research introduces a smart walker as a solution. The unique aspect of this study lies in its ability to address multiple issues through a single system. By taking into account the needs of caregivers and nursing homes, as well as eliminating the need for additional operating skills during use, the smart walker offers a holistic approach to mobility assistance. Furthermore, the functions and findings of this study can be extrapolated to other walking aids, opening up a myriad of potential applications. The versatility and adaptability of the smart walker suggest a promising future for enhancing mobility and independence for individuals in need.

1.3 Outline of the Thesis

The structure of this thesis is as follows. Chapter 2 provides an overview of existing research on walking support and smart walkers, positioning this study within the current landscape. Chapter 3 delves into the specific challenges that smart walkers must address, outlining key considerations and introducing a novel smart walker system. Chapter 4 delves into the analysis of the optimal level of support required by users, proposing a dynamic support decision-making method to maintain target speeds. Chapter 5 explores the importance of adapting user actions based on environmental cues and walking speed, presenting a collision avoidance algorithm that utilizes depth images from a stereo camera. In Chapter 6, a comprehensive summary of the thesis is provided. Chapter 3 draws from content published in a journal article [19]. Chapter 4 is based on the content published in [20, 21]. Chapter 5 is based on the content published in [22].

Chapter 2

Literature Review

2.1 Physical Benefits of Walking and the Need for Support

Walking is a fundamental form of human movement that holds significance not only for the elderly but for individuals of all ages. Walking is essential in maintaining and improving physical function and social skills.

From a physical health perspective, walking contributes to the preservation of muscle strength in the lower extremities and aids in the prevention of various diseases. Utilizing walking aids to facilitate movement helps in averting a decline in bone density, thereby effectively preventing conditions, such as osteoporosis and a deterioration in cardiopulmonary function [23]. Moreover, walking is effective for improving depression, depressive states [24], and blood pressure control [25]. A decline in walking ability can lead to escalated medical expenses, imposing financial strain on individuals and burdening the national healthcare system [26]. Sustaining both physical and mental well-being fosters a sense of motivation to engage in social activities, fostering positive relationships and interactions. The ability to move independently on one's feet facilitates access to various activities, such as shopping, hobby activities, and social interactions.

The pivotal role of walking in enhancing human health and quality of life is evident. Therefore, advocating for walking support is imperative, emphasizing the promotion of independent walking through the use of aids that ensure caregiver safety. However, Japan faces a critical shortage of caregivers [27], exacerbating the burden of care work [28, 29] is a serious problem. In this situation, the provision of walking aids that enable independent use assumes heightened importance. The demand for walking aids is expected to persist as a means of alleviating caregiver burden and fostering the autonomy of the elderly and individuals with physical impairments.

2.2 Technological Advances for Walking Aids

In response to the needs of an aging society, significant progress has been made in the engineering development of walking aids. One common walking aid, canes, has seen notable advancements.

Compared with other walking aids, canes are lightweight and compact, making them highly portable and effective for use in small living spaces. Various functions of canes, such as fall detection using the center of pressure-based method [13], three-wheel omnidirectional mobility [30], and estimation of walking intention using torque [31] have been implemented. These functions are crucial for ensuring stability for individuals requiring assistance while walking.

Recently, wearable exoskeletons [32, 33, 34] have emerged as a new walking aid, offering benefits, such as increased walking distance and improved muscle strength. However, in clinical practice, they have not been widely adopted owing to challenges related to wearing and cost considerations. The cost of mobility aids has been highlighted as a significant factor in a literature review [35].

Furthermore, the importance of proper training in the use of walking aids has been emphasized [36, 37], as inadequate training may exacerbate problems. Therefore, when proposing a walking aid with a new shape, improved convenience should be considered, as well as the similarity of operability with conventional walking aids.

Research by Pippin et al. [38] revealed that the appearance of mobility aids and social stigma serve as significant barriers to the acceptance and utilization of these devices, as indicated through 22 semi-structured interviews.

Based on the aforementioned findings, solely concentrating on enhancing patient safety or reducing the burden of walking may pose challenges in clinical practice. When developing an optimal walking aid, the user's walking difficulties, environment in which it will be utilized, and impact on caregivers must be considered from various perspectives.

2.3 Walker's Issues and Major Approaches

The structure of a walker ensures excellent safety by maintaining the center of gravity of the user within the base of support of the walker. In a study conducted by Fujita et al. [39], the influence of different walking aids on the walking capabilities of 10 residents in a healthcare facility was examined. The experiment involved multiple walking trials under three conditions: a forearm support walker, four-wheeled walker with a grip, and Rollator. The results indicated that the forearm support walker exhibited superior performance in key walking parameters, such as maximum walking speed, step length, and cadence.

Despite the advantages offered by walkers, many individuals who could benefit from their support do not utilize them. This reluctance is attributed to various factors related to the users themselves, caregivers, and the environment in which the walkers are used. To address these specific issues, a systematic analysis through clinical setting surveys and user questionnaires is essential.Furthermore, a tailored approach must be adopted in the design of smart walkers to effectively address each issue.

This research focuses on the utilization of walkers in nursing homes where multiple people reside together. The primary issues within this setting are as follows: the challenge of preparing a walker for shared use, the increased propulsion force owing to the walker's weight, and the necessity of preventing falls resulting from collisions and other factors. The research will explore various approaches to address these concerns.

2.3.1 Autonomous Navigation Function

Autonomous navigation involves the capability of a robot to navigate to its destination using visual sensor technology while avoiding obstacles and contact with individuals. This technology has been extensively investigated in fields, such as electric wheelchairs [40, 41, 42] and mobile robots, and autonomous navigation systems utilizing QR codes, which are gaining attention for their cost-effectiveness and high performance. However, the limitation of this method lies in the requirement to install QR codes and other landmarks on the ceiling and floor in indoor environments. Conversely, advancements have been made in autonomous wheelchair navigation technology using LiDAR and Kinect cameras [43]. Research is also underway on autonomous navigation using stereo cameras in diverse application fields, including unmanned aerial vehicles [44, 45], self-driving cars [46, 47, 48], and mobile robots [49, 50, 51].

This study delves into the development of a walker featuring autonomous navigation capabilities, equipped with a stereo camera based on cutting-edge technology. The primary objective of this innovative walker is to alleviate the preparation burden for the individual under care, while simultaneously promoting their independence. Moreover, this system is anticipated to lessen the workload of the caregiver. The autonomous navigation feature ensures that the user does not need to keep track of the walker's location, eliminating concerns about where to store it after use and potential negative reactions from others [35]. In nursing care facilities, there are places where it is difficult for autonomous mobile robots to move, such as carpets and small steps. This problem can be addressed by setting up areas where it is not possible to move, as is also done with conventional mobile robots. By incorporating autonomous navigation, the walker transcends its conventional role as a mere mobility aid, emerging as a pivotal solution that eases the psychological and physical strain in nursing care environments, ultimately enhancing the quality of life for the individual under care.

2.3.2 Propulsion Assistance by Motor

Motor-assisted propulsion is a prevalent feature of smart walkers. These walkers can be categorized into two types: those requiring user intervention and those operating autonomously. Walkers necessitating user intervention are characterized by a system enabling the user to regulate the motor's propulsion force and movement direction through an input device. Specific examples include devices that utilize joysticks [52] or handle-bars with embedded two-axis sensors [53]. Conversely, walkers operating autonomously detect the user's physical movements, environmental cues, and changes in speed, adjusting the motors accordingly. A cutting-edge system has been proposed for smart walkers, incorporating LiDAR technology to capture images of the user's lower body. This system is designed to detect when the user's foot leaves the floor, enabling precise control of the walker's motor [54]. Other smart walkers have been developed that utilize infrared sensors to monitor the movement of the lower limbs. These sensors adjust the speed and direction of the walker based on the walking pattern [55, 56]. These smart walkers, which do not require additional operations, also contribute to not increasing the cognitive load of the user.

Smart walkers that do not require additional input from the user are crucial for individuals, particularly the elderly, who may struggle with cognitive overload. A survey conducted with walker users revealed that older individuals often believe that motor-equipped smart walkers are challenging to use [57]. Notably, features that necessitate additional operations beyond those of conventional walkers could impede their adoption in clinical settings. This study focuses on utilizing the speed acquired by the hall sensor attached to the brushless DC motor as the sole input value to determine the propulsion force of the walker. The goal is to develop a walker that eliminates the need for users of traditional walkers to acquire new operating skills. By utilizing simple sensors for speed measurement in smart walkers, a multitude of applications are anticipated.

2.3.3 Collision Avoidance Function Using Visual Sensors

While walkers reduce the burden of walking for users, they also increase the risk of falling. In particular, backward falls while moving are reported to occur frequently [16]. Although walkers are recommended in clinical practice to reduce the risk of falls in the elderly [58], it has been shown that there is no significant difference in the incidence of falls between walker users and non-users [59].

A primary factor contributing to falls is the loss of balance while walking, often resulting from sudden changes in speed caused by collisions. These collisions can be prevented by implementing visual sensors to detect obstacles ahead of time. By proactively avoiding collisions with obstacles, the risk of falling can be significantly reduced. As such, this study is dedicated to exploring collision avoidance mechanisms that leverage visual sensors.

A method that utilizes an RGB-D camera to obtain distance information on obstacles and then transmits this information to the user through a tactile sensor was proposed [60]. Another method [61] involved the utilization of a combination of a laser distance and sonar sensors to scan the area ahead, determine a safe path based on the meandering angle, and navigate to a secure location utilizing a motor attached to the front wheel.

In this study, a collision avoidance function is introduced that utilizes depth images from a stereo camera to identify obstacle direction and prevent collisions by decelerating the motor. The performance of avoidance actions using depth images in a smart walker with forearm support has not been extensively validated. Objects that may collide within a nursing care facility include the walls of corridors and other areas, caregivers, facility users, and installed furniture. In this study, we will focus on objects that are not particularly dangerous but are frequently approached, such as walls and low-height installed objects. Therefore, the purpose of this study is to assess the effectiveness of the proposed collision avoidance function for these objects through performance evaluation.

Chapter 3

Development of Smart Walker System with Autonomous Navigation

3.1 Introduction

While walkers provide enhanced stability owing to their large base of support, several challenges must be addressed prior to their utilization. Care recipients must easily access the walker when needed. However, unlike other mobility aids, such as canes, walkers occupy substantial space, limiting spatial flexibility when placed nearby. This has led to concerns in care facilities about walkers obstructing the paths of others [35]. One potential solution to this issue is to position walkers in remote shared spaces. However, this would require caregivers to transport the device each time, potentially impacting the independence of care recipients. With Japan currently facing a shortage of caregivers, implementing systems that add to the workload of care facilities presents significant challenges.

In recent years, the demand for service robots equipped with autonomous navigation capabilities has increased. These robots eliminate the need for human intervention in object transportation and gained popularity during the global COVID-19 pandemic for their ability to minimize human contact. The advantages of service robots extend beyond contactless operation to include reduced staff workload, which is particularly crucial in caregiving environments. This study proposes the development of a smart walker that maintains the conventional forearm support design while incorporating autonomous navigation functionality.

LiDAR systems are commonly employed in conventional autonomous navigation systems; however, this research focuses on stereo cameras characterized by high spatial resolution and energy efficiency. Previous studies have not thoroughly evaluated the autonomous navigation capabilities of forearm support walkers equipped with stereo cameras. The implementation utilizes a robot operating system (ROS), a versatile robotics platform, to conduct real-world navigation experiments and assess the practical applicability of autonomous navigation in care facility corridors, using path deviation rates as performance metrics.

The remainder of this section is organized as follows. Section 3.2 outlines the system design of a smart walker with autonomous navigation functions, Section 3.3 details the experimental setup and results to validate the effectiveness of the autonomous navigation functions, and Section 3.4 provides the conclusion.

3.2 Overview of the Proposed Smart Walker

This section delves into the use case scenarios and system configuration of the proposed smart walker, focusing on the necessary hardware components (frame structure, sensors, and actuators) and the software implementation of the motor control system.

3.2.1 Usage Scenarios

The walker developed in this study is intended for individuals requiring light nursing care to navigate a care facility independently. The system is designed to deliver the walker to the user without requiring assistance from caregivers, support the user's walking by assisting with motor control, and display the route to the destination. Additionally, the functional design and mode of operation of the walker are explored to accommodate multiple users. An example of a scenario in which a person that supposed to use a walker requires a sink is shown in Figure 3.1. The detailed flow of the scenario is as follows:

1. The user initiates a call to the walker by pressing a button on their bed in the nursing home.

2. The walker autonomously drives from the waiting area to the user's room.

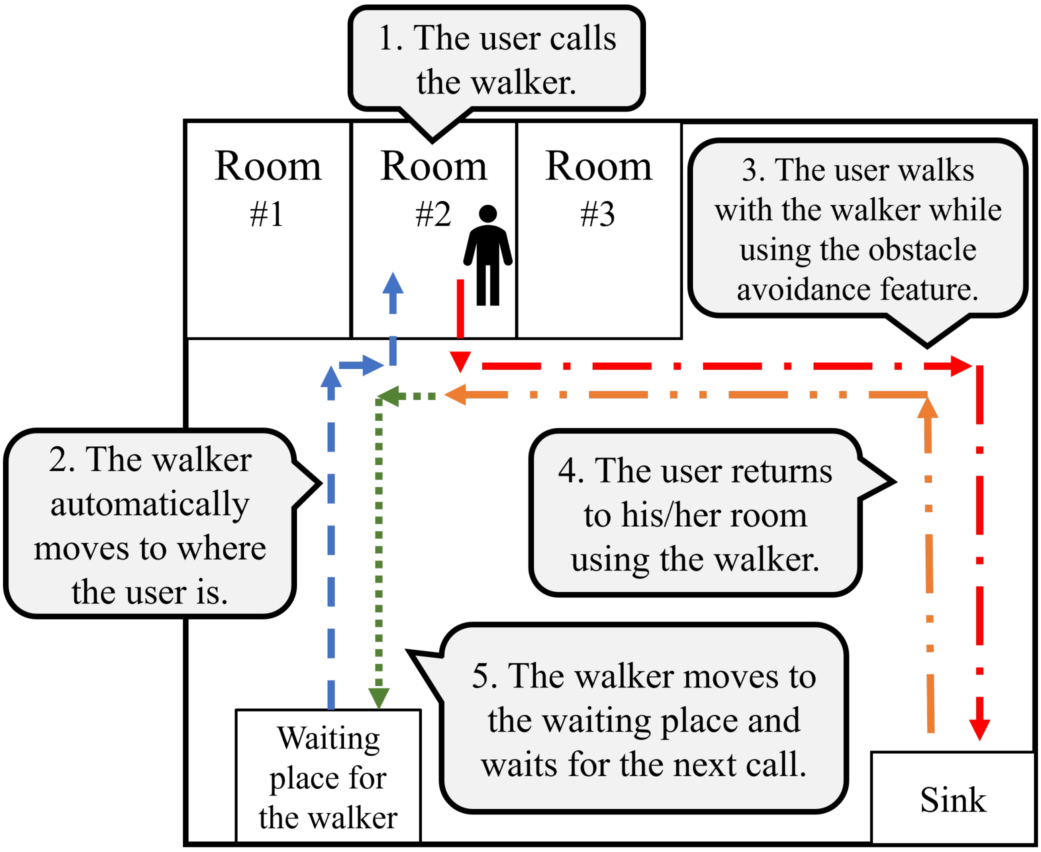

Figure 3.1: Example of the application scenario of the walker.

3. The user is assisted by the walker to reach the sink using its walking support function.

4. After using the sink, the user is guided back to their room by the walker.

5. Once the user reaches their room, the walker returns to the waiting area and remains there until the next call.

3.2.2 Frame of the Walker

In this study, we modified an existing forearm support four-wheeled walker by removing the rear wheels and installing tires connected to a brushless DC (BLDC) motor. A forearm support quadruped walker, shown in Figure 3.2, is a type of wheeled walker, where the forearm is placed on a holder at a 90 ° angle to support the user's body weight. This walker provides optimal stability during movement and can change its direction by rotating the casters. The dimensions of the forearm support four-wheeled walker frame are 630 mm wide, 730 mm deep, and adjustable in heights from 1000

(a) Metal walker utilized in the experiment.

(b) Condition in which the body weight is supported.

Figure 3.2: Forearm support four-wheeled walker utilized in experiments.

to 1250 mm. The total weight of the walker without sensors or actuators is 9.7 kg, with rubber wheels measuring 145 mm in diameter.

3.2.3 Sensors and Actuators

The devices attached to the walker, utilized in this study, are listed in Table 3.1, whereas the input and output of each device attached to the walker are shown in Figure 3.3.

A list of the sensors attached to the walker is shown in Table 3.1. The inputs and outputs of each device attached to the forearm support four-wheel walker are shown in Figure 3.1. The ZED 2 [62], a stereo camera commercialized by Stereolabs, is a cutting-edge device capable of capturing depth images and equipped with sensors, such as an IMU and a barometer. In this study, we aim to implement autonomous navigation features utilizing SLAM technology for obstacle avoidance, leveraging depth images and position tracking technology. The NVIDIA Jetson Nano [63], an embedded single-board computer developed by NVIDIA, is essential in this study. We will collect and process the data from ZED 2, transmitting signals to Arduino UNO through an SSH connection. The Arduino UNO R3 [64], featuring an AVR microcontroller and various input/output ports, is connected to a BLDC motor driver

Table 3.1: Devices attached to the walker.

Device	Number of units
ZED 2	1
NVIDIA Jetson Nano Developer Kit	1
Arduino Uno Rev3	1
Brushless DC Motor	2
Motor driver (TB6605FTG)	2
Battery (Anker PowerCore Essential 20000)	2
Wheel	2

to regulate the rotation direction and speed of the left and right wheels. Control of the motor's speed is achieved through the duty ratio of the PWM output from the Arduino UNO, which adjusts based on the voltage applied to the BLDC motor. The PWM signal frequency was set at approximately 490 Hz. In the case of the Arduino UNO, when the duty ratio is set to 0%, the output voltage is 0 V, and at 100%, it is 5 V. Power is supplied by a 12 V 1 A battery for the BLDC motors and a 5 V 3 A battery (Anker PowerCore Essential 20000) for the Jetson Nano. Autonomous navigation to the user's location is achieved by controlling the motor's rotation direction and torque using an Arduino UNO and a brushless DC motor driver. The user walking support function detects the direction of rotation of the wheel using the hall IC mounted on the BLDC motor, ensuring the motor rotates in the correct direction.

3.2.4 ROS Control

The autonomous navigation function of the proposed system is communicated through topic communication in the ROS, which is a software platform for robots. The version to be utilized is ROS melodic (1.14.10). To enable autonomous navigation for the walker, we implemented the Navigation Stack package. This package generates speed commands for the robot based on sensor information, allowing it to efficiently navigate to the target point. The interface for sending commands was established using rviz, a 3D visualization tool within ROS. Real-time appearance-based mapping (RTAB-Map) [65, 66, 67] was adopted to create the map. An image of the actual room in which the experiment was conducted is shown in Figure 3.4, whereas a map of the room and hallway created utilizing the stereo camera and RTAB-Map is shown

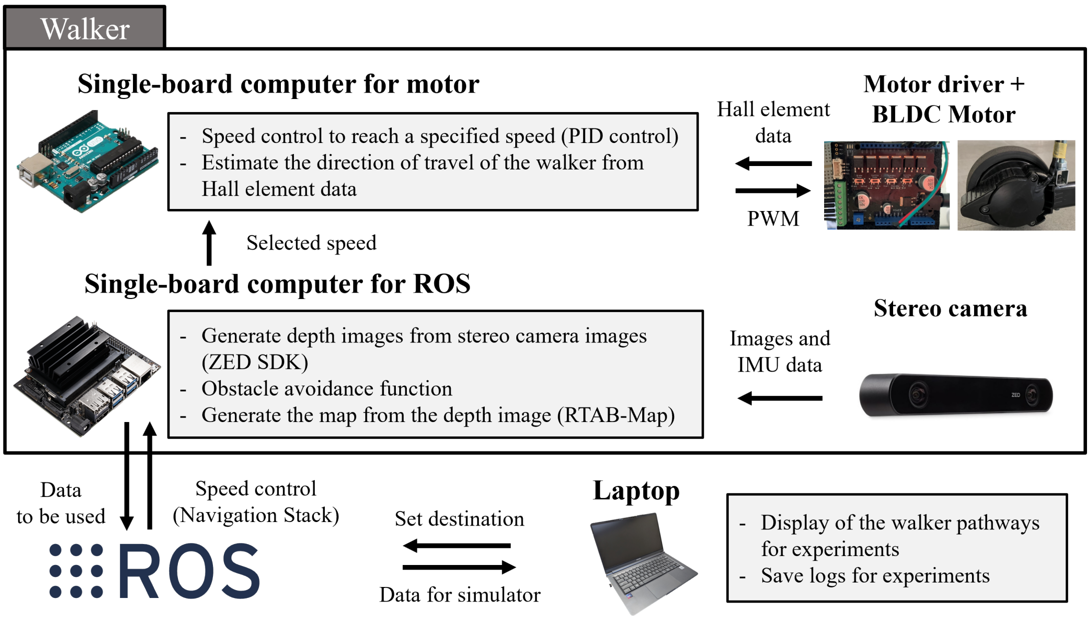

Figure 3.3: System schematic.

Figure 3.4: Experimental location.

in Figure 3.5. Furthermore, the zed-ros-wrapper published by Stereolabs was utilized to communicate the ZED 2 sensor information to the ROS. The versions of ZED SDK and zed-ros-wrapper to be installed on Jetson Nano are 3.4 and 3.2, respectively.

3.2.5 Motor Control

For autonomous navigation, the navigation stack requires three-axis speed and three-axis angular velocity to guide the robot to the target point. Therefore, the micro-computer connected to the motor must be capable of moving at specific speeds and

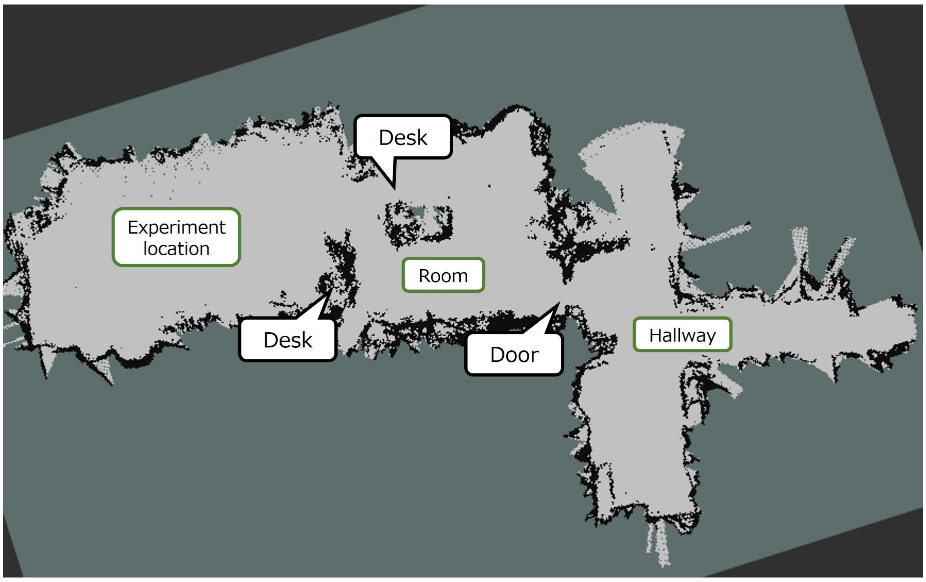

Figure 3.5: Map shown in rviz.

angular velocities. We implemented PID control [68] for speed regulation on the motor side. The PID control formula is expressed as follows:

$$u(n) = K_p e(n) + K_i \sum_{k=0}^{n} e(k) + K_d(e(n) - e(n-1)) \tag{3.1}$$

where K_p represents the proportional gain, K_i represents the integral gain, and K_d represents the differential gain. $e(n)$ represents the error at time n (the difference between the target and current speeds in this context). The parameters were adjusted manually to reduce overshooting.

3.3 Experiments on Autonomous Navigation Function

In this experiment, we validated the accuracy of autonomous navigation at the target point.

3.3.1 Experimental Settings

First, we validated the fundamental movements necessary for autonomous driving toward the target point. These movements include turning and forward motion. To assess the turning movement, we recorded the camera position and angle when the walker was instructed to make a 90° turn. For the forward movement, we recorded the self-position of the walker when the target point was set at a distance of 5.0 m

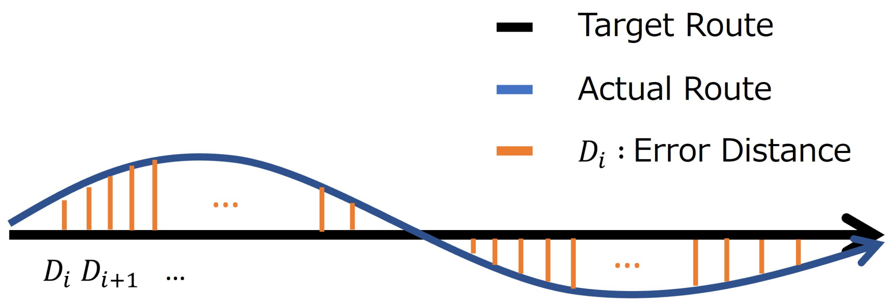

Figure 3.6: Error distance calculation for XTE.

ahead. Subsequently, we performed autonomous navigation along a predetermined route. During forward movement and route traversal, we output the cross-track error (XTE), which indicates the discrepancy between the target and actual routes. XTE is expressed as follows:

$$XTE = \frac{1}{N}\sum_{i=1}^{N} D_i, \tag{3.2}$$

where N denotes the number of measurement points and D_i denotes the error distance between the target and actual routes. We conducted ten tests and computed the average XTE to assess the stability and accuracy of autonomous navigation. A simplified diagram of the error distance D_i utilized in XTE is shown in Figure 3.6.

3.3.2 Results and Discussion

The turning motion on rviz is shown in Figure 3.7. The start and directions of the arrow denote the current position and direction of the walker, respectively. As shown in Figure 3.7, a precise 90° turn was achieved. Table 3.2 shows the results of all forward movements and route runs. The average XTE of forward movement was 0.052 m, with a driving route exhibiting an XTE of 0.060 m, as shown in Figure 3.8. Our findings indicate that the walker consistently remained within 1.0 m of the target route, albeit some minor twisting movements were observed. The average XTE of the route run was 0.246 m. The driving route with an XTE of 0.254 m is shown in Figure 3.9.

During the course of the journey, the walker came in close proximity to the four corners of the square. However, a significant deviation from the intended route occurred when transitioning from forward to turning movement. The limited accuracy of the self-position estimation system utilizing the stereo camera prevented the com-

Table 3.2: XTE results of forward movement and route run.

Test Number	Forward XTE [m]	Route XTE [m]
1	0.071	0.192
2	0.028	0.254
3	0.010	0.368
4	0.020	0.273
5	0.002	0.316
6	0.125	0.213
7	0.002	0.191
8	0.109	0.251
9	0.042	0.186
10	0.060	0.211

plete elimination of the walker's meandering motion.

Our proposed walker is intended for use in facilities, such as hospitals and nursing homes. These facilities are characterized by spacious corridors and rooms in which the walker is expected to operate. Additionally, these environments typically do not experience high densities of walkers or facility users.

In light of these facility characteristics, three operational policies are recommended:

1. Avoid autonomous operation of the walker in narrow pathways
2. Refrain from using the walker in crowded settings
3. Maintain distance between multiple walkers to prevent interference.

Adherence to these operational policies is expected to ensure smooth operation of the walker.

Furthermore, to enhance the accuracy of the walker's self-positioning, two potential causes of meandering driving have been identified. First, the positional relationship between the two motors was not clearly defined within the ROS framework. Second, reliance solely on the stereo camera for self-position estimation may not satisfy the required accuracy for independent operation. This issue can be addressed by incorporating wheel rotation information for odometry-based self-position estimation.

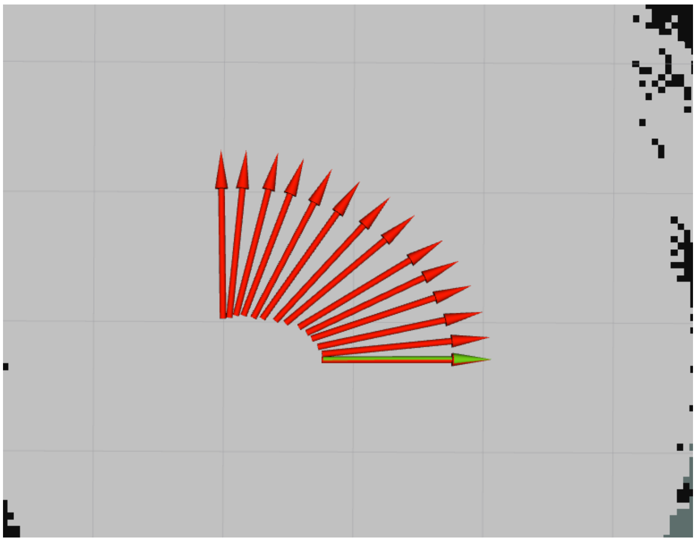

Figure 3.7: Camera position and angle during right turn.

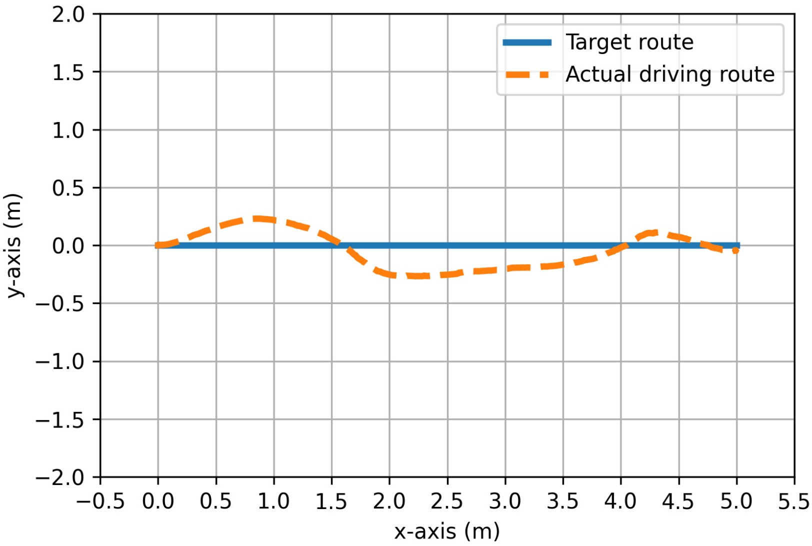

Figure 3.8: Target and actual route during forward movement.

3.4 Conclusion

In this chapter, we proposed a smart walker system with autonomous navigation capabilities to address a major challenge of walkers: the cumbersome task of preparing the walker for use. Recognizing the size limitations associated with traditional walkers, we have developed our system using compact devices to ensure practicality and ease of use. Subsequently, we conducted autonomous navigation experiments to validate the overall system feasibility and effectiveness of the autonomous navigation

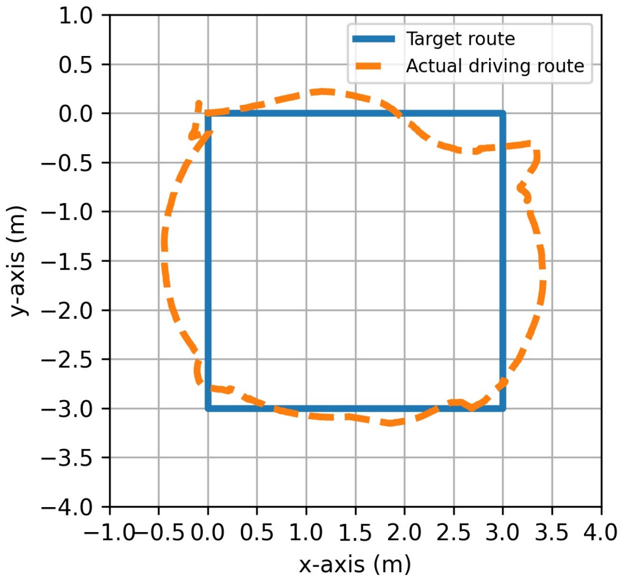

Figure 3.9: Target route and routes during driving.

function. These experiments involved assessing goal achievement by measuring the error distance between the final target and stopping positions, as well as evaluating the accuracy of autonomous navigation through the cross-track error analysis. Our results demonstrated that the smart walker's autonomous navigation function successfully reached specified target points, although some minor meandering was observed during circular route navigation. To address this issue, we are exploring potential solutions, such as incorporating rotation information from both wheels for improved self-localization and enhancing computational capabilities to reduce response time. We demonstrated that the stereo camera-based autonomous navigation system achieved sufficient accuracy in environments with wide corridors where slight meandering is acceptable.

Furthermore, while we utilized stereo cameras for depth image estimation in this study, monocular camera-based depth imaging [69, 70] is also feasible with adequate computational power. Our proposed depth image-based system can leverage advancements in image processing research, paving the way for future space optimization and enhanced functionality.

Chapter 4

Effect of Support Amount on Motorized Support for Walking

4.1 Introduction

The walker significantly contributes to maintaining balance during walking. Its wide base of support design allows users to achieve and maintain stable standing postures by ensuring that their body's center of gravity consistently remains within the base of support. This high level of stability makes it a valuable tool in clinical rehabilitation settings, serving as an effective assistive device that promotes mobility independence, particularly for elderly individuals with limited walking ability and patients with physical frailty.

Despite its benefits, walkers do face challenges. Issues such as excessive weight and operational complexity can be problematic for users. Shin et al. [71] investigated the willingness to switch to a developed smart walker among 23 nursing home residents, revealing that increased walker size and weight led to decreased acceptance rates. This highlights the importance of optimizing weight and size when designing walkers to ensure they are well-received by their intended users.

While incorporating propulsion assistance functions into walkers is common to address weight concerns, several limitations exist. Assistive suits wearable mobility assistance devices can enhance walking ability but may pose challenges in terms of usability. Smart walkers often utilize motor-based propulsion assistance, with commercial products available on the market. However, while smart walkers implement advanced functions, it has been noted that users must learn new skills [35], and they are reluctant to transition to walkers requiring new operational methods [71].

To validate the effectiveness of propulsion assistance systems, establishing objective evaluation metrics is essential. Surface electromyography (sEMG) has become a widely adopted method for this purpose, as it provides a non-invasive and quantitative assessment of muscle contraction intensity. sEMG works by detecting and amplifying action potentials generated during muscle cell contraction from the body surface, with applications spanning rehabilitation and sports science. Previous research in the field of walking assistance devices has focused on various devices, including shopping carts and forearm support walkers [72]. However, these studies have been limited to fixed assistance levels, where a constant propulsion force is applied through motor torque. This study attempts to identify the most effective assistance parameters for reducing muscle activity by conducting sEMG measurements under multiple assistance level conditions. By doing so, we seek to identify the optimal support levels for forearm support walkers more objectively and quantitatively compared with conventional subjective evaluation.

The level of propulsion force required in walking assistance devices varies based on dynamic factors, such as user walking speed and target velocity. Optimal assistance levels also depend on individual users' normal walking speeds and weight-bearing capacities. This study develops a mathematical model to describe the mechanical interaction between forearm support walkers and users. Through theoretical analysis, we aim to understand how assistance levels vary under different usage conditions and propose an adaptive assistance level determination method based on these insights.

This research proposes a novel assistance level determination algorithm for walking support devices. The proposed method utilizes motor velocity information commonly installed in such devices and can be implemented without significant modifications to existing walker frames. In the evaluation experiments, quantitative assessments of tracking performance and stability relative to target speeds will be conducted through basic experiments using weights simulating constant loads, followed by empirical validation through subject experiments.

The remainder of this section is organized as follows. Section 4.2 examines the relationship between the forces generated during walking in numerical terms. Section 4.3 describes the ideal support in this study and explains the algorithm for determining the dynamic support amount. Section 4.4 presents the validation results using questionnaires and sEMG measurements. Section 4.5 demonstrates the tracking and stability of the proposed dynamic support amount through weighted experimental trials. Section 4.6 presents the results of subject experiments using the proposed support amount algorithm. Finally, Section 4.7 concludes the chapter.

4.2 Forces Generated when Walking with Smart Walker

The level of support needed by users of smart walkers is a dynamic and intricate component. This support fluctuates continuously, depending on the force exerted by the user on the walker and their walking speed. This support should be adjusted accordingly to accommodate the user's walking condition. In our research, we establish the optimal support level as the motor torque necessary to sustain the user's desired walking pace, promoting prolonged and effective walking.

The method of providing support varies widely depending on the design of the smart walker. Walkers equipped with input devices, such as handles detect pressure or tilt transmitted to these devices to determine the amount of support provided by motors mounted on the tires. Conversely, walkers lacking input devices typically offer a fixed amount of support in the direction of movement. However, the actual support required during walking is a complex function that changes dynamically based on the relationship between motor speed, torque, and force applied by the user to the walker.

To comprehend the primary force relationships at play when utilizing a forearm support walker, a side view of the user and the smart walker is shown in Figure 4.1. This force distribution is influenced by various factors, such as the floor and frame materials, as well as the positioning of the user's forearms. This study aims to identify variables that determine the optimal level of support during walking, rather than delving into intricate physical modeling. To streamline this analysis and extract the fundamental force relationships, we set the following conditions for illustration:

- The rolling friction force is equal for all tires
- The weight on all tires is equal
- No forward or backward slippage exists between the user's forearm and support platform

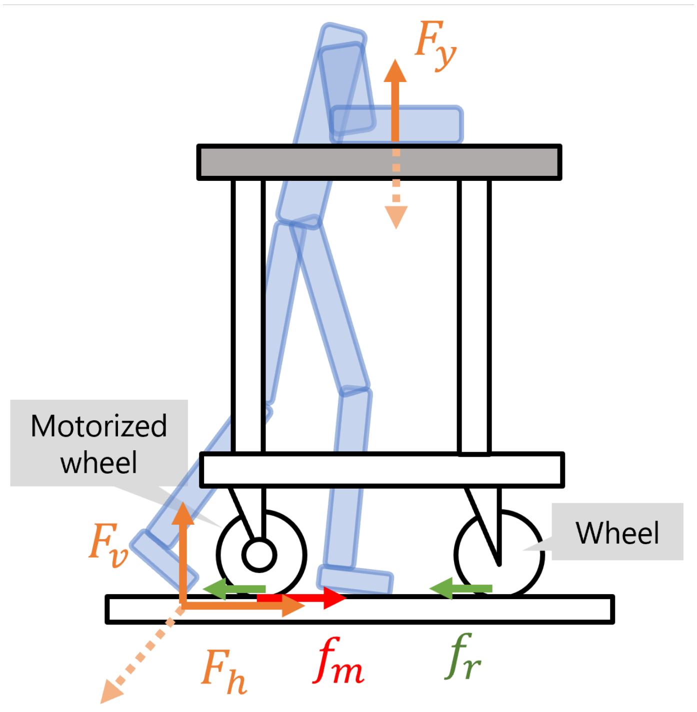

Figure 4.1: Primary forces at play when walking with a forearm support walker.

To understand the mechanical behavior of the smart walker, we define each physical quantity using the coordinate system shown in Figure 4.1. The right direction is defined as forward, with positive values assigned to physical quantities in this direction, whereas the left direction is considered backward and given negative values. The horizontal velocity v of the walker typically ranges from $\pm$ 1.5 m/s considering walking speeds. Air resistance acting on the walker is deemed negligible compared with other forces and is therefore not considered in this analysis. The primary forces involved in walking include the ground reaction force, which can be decomposed into F_v and F_h. F_v represents the vertical force for body weight support, whereas F_h represents the horizontal force for propulsion. Additionally, F_y denotes the force generated by placing the forearm on the forearm support, which widens the support base and enhances postural stability. An increase in F_y results in a decrease in F_v, reducing the strain on antigravity muscles. A significant force influencing the movement of walkers is the rolling friction force f_r, which occurs at the contact surface between the tires and floor. It is expressed as follows:

$$f_r = \mu_r(mg + F_y) \tag{4.1}$$

where μ_r represents the rolling friction coefficient, m represents the mass of the walker, and g represents the gravitational acceleration. The BLDC motor, responsible for propulsion, converts electrical energy into mechanical energy. The torque generated by the motor provides rotational force to the wheel, which is converted into propulsive force f_m through friction with the ground. This relationship is expressed as follows:

$$f_m = kP/v \tag{4.2}$$

where P represents the controlled power, v represents the velocity, and k is a coefficient that denotes the motor's conversion efficiency. The walker utilized in this study is a rear-wheel drive, with the motor's propulsive force acting solely on the rear wheels. The power P is adjusted by altering the duty cycle through PWM control.

These relationships offer valuable insights into the mechanical behavior when using a smart walker. As shown in Equation (1), increasing F_y for body weight support also increases the rolling friction force in the opposite direction of movement, necessitating a greater propulsive force. Based on Equation (2), the motor's torque changes based on the current walking speed v. These analysis results indicate that the level of support required during walking varies based on the user's condition and walker's state. Therefore, this study aims to implement a support adjustment function that adapts to these varying support requirements and maintains the ideal walking speed.

4.3 Ideal Support and Adopted Support Volume Algorithm

In this research, ideal support refers to assistance that enables users to maintain their individual ideal walking speed regardless of the pressure exerted on the walker. Research by Holt et al.'s research [73] suggested that individuals enhance their energy efficiency and stability when walking at their desired pace. Achieving this ideal support necessitates precise motor control of the smart walker. Precisely adjusting the speed of the left and right tires allows for both straight movement and curved direction changes. This capability enhances navigation to the destination by predicting the shortest route typically chosen by humans and adjusting tire speeds accordingly, providing more natural and efficient walking support.

To achieve this level of support, we have developed a motor control system that utilizes incremental PID control. This system enables precise and adaptive speed adjustment based on the user's walking characteristics. The adoption of incremental PID control was driven by the need to reduce computational demands when performing calculations on the Arduino Uno, thereby minimizing response delays. Moreover, it offers the advantage of maintaining stable control even when the speed measurements obtained from the Hall sensor contain outliers. The control algorithm is expressed as follows:

$$MV_n = MV_{n-1} + \Delta MV_n \tag{4.3}$$

$$\Delta MV_n = Kp(e_n - e_{n-1}) + Kie_n + Kd((e_n - e_{n-1}) - (e_{n-1} - e_{n-2})) \tag{4.4}$$

The control variable is the PWM duty ratio, which allows for the adjustment of the current supplied to the motor. The target value is the ideal walking speed set for each user, with the input being the actual speed calculated from the Hall sensor attached to the motor. MV_n represents the current (time n) duty ratio, whereas MV_{n-1} represents the duty ratio from the previous step. e_n represents the deviation between the target and current speeds, and e_{n-1} represents the deviation from the previous step. Kp, Ki, and Kd represent the coefficients for the proportional, integral, and derivative terms, respectively. To accommodate walker movements, such as changes in directions, the left and right motors are controlled independently. The parameters were calibrated in a real-world setting rather than a simulated one. Consequently, primary auto-tuning techniques were not employed owing to constraints, such as the maximum driving distance and floor surface area in the experimental environment. Each control coefficient was manually tuned and determined as $Kp = 0.03$, $Ki = 0.08$, and $Kd = 0.06$. This manual tuning was based on the following criteria:

- Ensuring no oscillation when the speed stabilizes at the desired speed
- Limiting the maximum speed overshoot to 1.5 times the desired speed even when the load on the smart walker fluctuates.

Particular emphasis was placed on suppressing oscillations during speed stabilization. While completely eliminating overshoot presented a challenge, we were able to achieve a level within an acceptable range. The speed measurement utilizing the proposed Hall sensor required a minimum rotation angle of 51.43° . To initiate movement from a standstill, fixed duty ratio torque control was employed. Once speed measurement became feasible, the transition to PID control was implemented. Settling time minimization was not a focus of this tuning process, as the acceleration at the start of walking can vary significantly based on the user and circumstances. The upper limit for the duty ratio of the control amount was set at 62.75%. A propulsive force exceeding this upper limit would result in the user receiving excessive propulsive force assistance from the smart walker, potentially compromising their normal stable walking posture.

4.4 Electromyographic Evaluation of Lower Limb Muscles under Different Support Amounts

The purpose of this experiment was to validate whether the walking support function at several support levels could reduce the walking load on the user. A reduction in walking load implies decreased muscle strain while utilizing the walker. The proposed walker drives its motors to generate forward force when the user initiates walking and pushes the walker. To provide optimal support, the rotation torque or assistance level must be calibrated to an appropriate value. Excessive assistance could lead to the walker moving forward autonomously. Consequently, users may attempt to slow down the walker, potentially increasing the walking load beyond normal levels. Walking engages many muscles in the lower limbs. In this experiment, we measured the electromyography values of five muscles in the lower limbs that are active during walking and evaluated the effectiveness of the walker's walking support function.

4.4.1 Experimental Setup

The muscles assessed were the peroneal muscle (PM), tibialis anterior muscle (TAM), gastrocnemius muscle (GM), vastus lateralis muscle (VLM), and biceps femoris muscles (BFM) of the right lower extremity. Owing to the challenge of simultaneously measuring muscle activity on both sides, we focused on the EMG of the right leg. The measurement setup is shown in Figure 4.2. A wireless surface electromyograph (TELEmyo G2, NORAXON) was utilized to measure the EMG. The sampling frequency was set at 1500 Hz, and the data were digitized and transferred to a personal computer. The data were processed with a 30-500 Hz band-pass filter and then processed using root mean square (RMS) with a window width of 100 ms. Subsequently, the data were normalized to the maximal voluntary contraction (MVC) value, with this value serving as the muscle activity index (%MVC). The maximum %MVC was recorded for each step, from the moment the right lower limb's heel touched down to the landing of the subsequent heel. Our study involved four participants, three in their 20s (A, B, and C) and one in his 50s (D), all without medical issues related to the ankle joint. Given that the walker under development targets individuals with mild nursing care needs who struggle to walk independently, the participants' walking abilities varied slightly. Therefore, to increase the walking load during the experiment, participants were equipped with a 10 kg weight vest, and a 12 kg weight was added to the walker. An image of the weighted walker is shown in Figure 4.3. The experiment was conducted in an indoor environment on a flat surface, with a focus on observing basic walking movements in a straight line. Participants were instructed to initiate walking with their right foot from a stationary position and to stop after covering a distance of 5 m. If the walking speed is unified, muscle activation changes for speed control, and muscle activity measurement during normal walking may be infeasible. Therefore, the participants were instructed to walk at normal walking speed.

To reduce the walking load, five trials were conducted at assist levels of 0 (OFF), 40, 100, and 160. The assist level corresponds to the duty ratio of the PWM signal provided to the motor. The ratio is 100% at the maximum value of 256. In other words, the duty ratio was approximately 15.6% when the assist level was 40. We conducted an experiment to analyze muscle activity levels during normal walking. We focused on the fourth step of the walking cycle, specifically excluding the acceleration and deceleration phases for our analysis. By analyzing the data collected, we determined the maximum %MVC for each muscle. These values were then normalized based on the %MVC recorded when the assistive device was turned OFF.

One defining characteristic of a walker is its consideration of the muscle forces exerted by the legs for propulsion, while the hands are utilized for pushing and support. These forces are contingent upon the weight the user places on the walker. To maintain a consistent weight distribution, we conducted exercises where users walked with approximately 10% of their body weight supported by the walker each time the level of assistance was adjusted.

4.4.2 Results

For each measurement muscle point of each participant, the median of the maximum %MVC of the five trials without assistance is utilized as the reference value. The

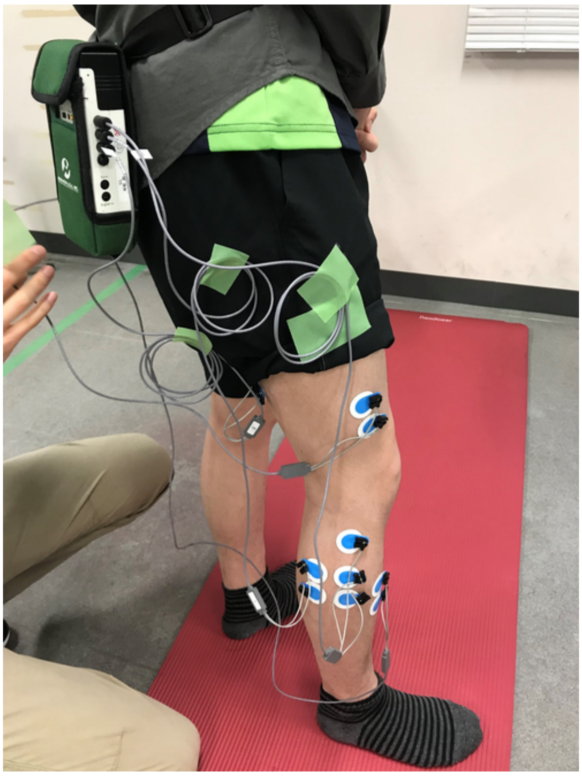

Figure 4.2: Appearance of myoelectric measurement.

Figure 4.3: Weight loaded walker.

ratio of the median of the maximum %MVC of each measurement point and participant with different levels of assistance to this reference value is calculated. This method is employed owing to variations in gait characteristics and maximum %MVC values among participants, making it difficult to discern overall trends based solely on %MVC. As a concrete example, the MEAN and SD of the VLM of each participant are listed in Table 4.1.

Notably, participant B exhibited more than double the %MVC compared with those of other subjects, highlighting significant variability in %MVC even within the same muscle group. Subsequently, the %MVC ratios for each participant were summarized and presented.

The results for participant A are shown in Figure 4.4, revealing decreased muscle activity in the PM and TAM muscles when utilizing the walking support function. Notably, a similar trend was observed between assist levels of 40 and 100. Participant A experiences reduced muscle activity in four out of five locations with an assist level of 160, particularly in the VLM.

The results for participant B, shown in Figure 4.5, indicate a decrease in %MVC for all measurement points except VLM when the walking support function was activated. Furthermore, the change in the level of assistance was insignificant, and it decreased uniformly. However, VLM exhibited an increase in %MVC with assist levels of 40 and 100, followed by a decrease at an assist level of 160. %MCV of VLM decreased as the level of assistance increased. The results indicated that %MVC at all measurement points were lower than the reference value when the level of assistance was 160.

The results for participant C are shown in Figure 4.6. The %MVC values for PM and GM activity increased at assist levels of 40 and 100 compared with values without assistance. However, for TAM, %MVC was lower than the standard value when utilizing the walking support function. Specifically, when the overall muscle activity decreased, the assist level was 100, three out of five locations showed lower values compared with the standard value.

The results for participant D are shown in Figure 4.7. Overall, the muscle activity of the five points measured decreased when the level of assistance was 40. Subsequently, %MVC increased from 100 to 160, with TAM %MVC exceeding the reference value at 100 and 160. Additionally, PM %MVC was higher than the stan-

Table 4.1: %MVC of the VLM for each subject.

Subject	Assist power			
	OFF	40	100	160
A	23.57 ± 2.58	21.15 ± 5.27	21.10 ± 7.09	11.97 ± 5.00
B	52.73 ± 10.45	62.04 ± 5.61	55.60 ± 9.46	51.13 ± 5.20
C	27.55 ± 3.46	22.87 ± 4.45	25.57 ± 2.43	27.18 ± 1.63
D	20.86 ± 5.18	18.87 ± 2.85	17.67 ± 2.45	20.71 ± 3.03

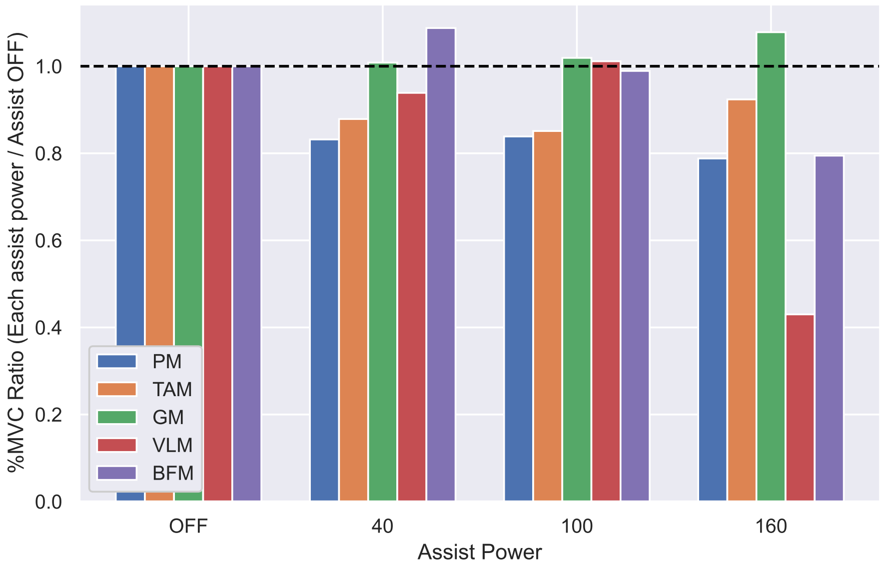

Figure 4.4: %MVC ratio for subject A.

dard value when the level of assistance was 160. The results indicate that %MVC for all muscles in the measurement area was below the standard value when the assist level was 40.

In post-experiment interviews, three out of four participants (A, B, and D) expressed feeling unsupported by the walker at an assist level of 40. All participants reported feeling most comfortable walking with an assist level of 100. At an assist level of 160, all participants felt as though they were being pulled forward by the walker. Participants A, B, C, and D reported that they could sense the walker continuing to move forward even when they stopped walking, requiring them to pull the walker to maintain its position, a sensation not experienced at assist levels below 160.

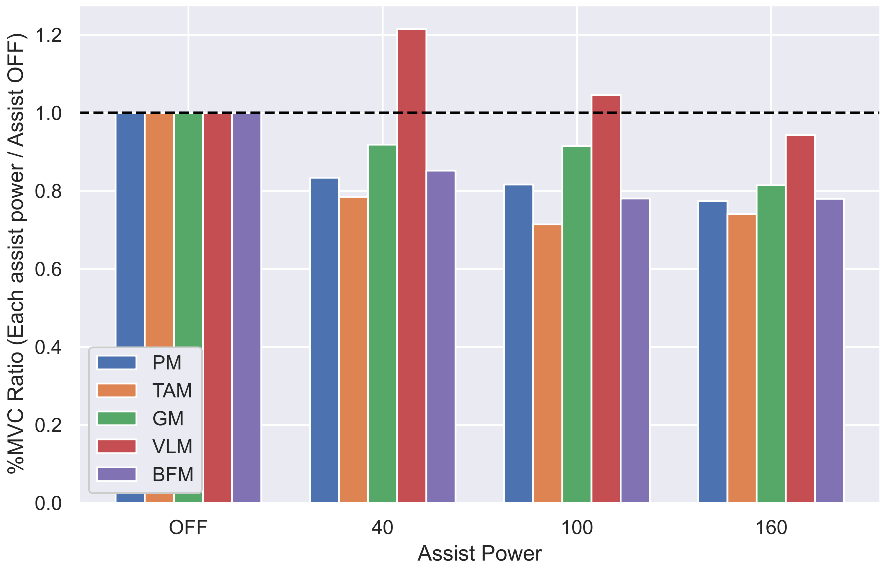

Figure 4.5: %MVC ratio for subject B.

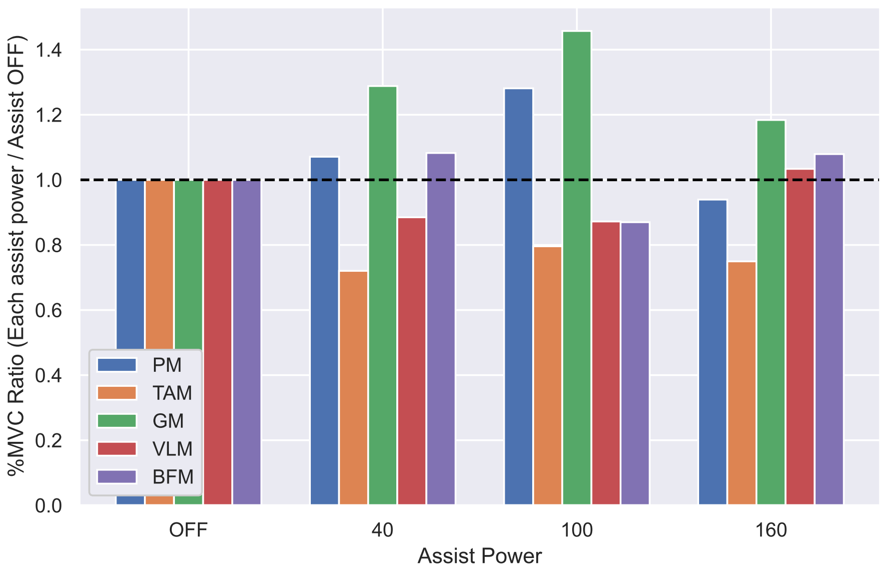

Figure 4.6: %MVC ratio for subject C.

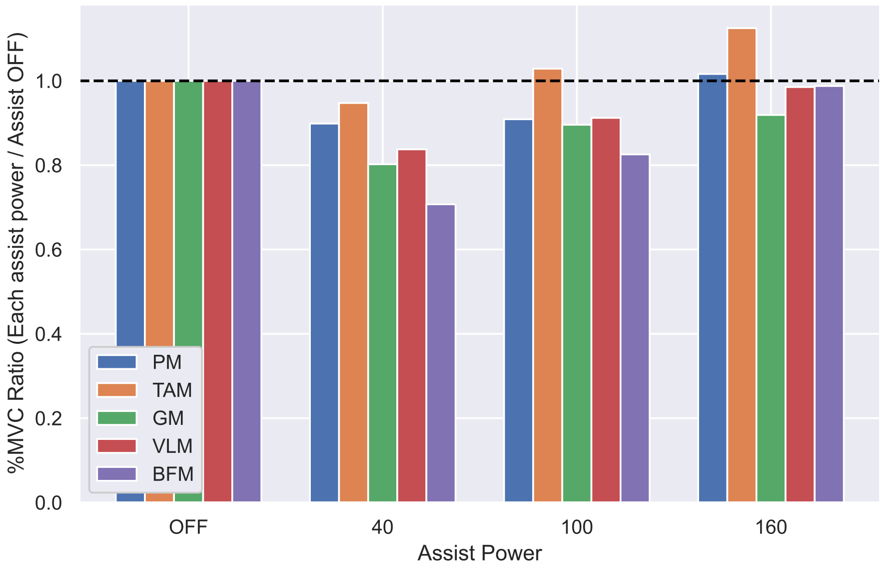

Figure 4.7: %MVC ratio for subject D.

4.4.3 Discussion

Through the experiments conducted, a noticeable trend emerged indicating that enabling the walking assistance function resulted in reduced overall muscle activity. However, for certain participants and levels of assistance, muscle activity at specific measurement points actually increased with the walking assistance. While the potential for reducing muscle load with the proposed walker has been validated, further experiments are necessary to determine whether this reduction results from EMG measurement noise, variations in walking gait among participants, or differences in the optimal amount of assistance for each individual.

Interviews with the participants revealed that they could only detect unintentional behavior of the walker when the assistance level exceeded 160. Despite this, the observed decrease in muscle loads occurred even when the assistance level was below 160, suggesting that the proposed walking assistance algorithm is safe for users as long as the appropriate level of assistance is provided.

To accurately assess the impact of walking assistance on muscle load, several methods can be considered in addition to increasing the number of participants and trials. First, in this experiment, the focus was on measuring the four steps of a 5-m walk. However, owing to the limited measurement period, conducting measurements for an extended period or distance was not feasible. To minimize the dispersion of EMG values and gain a comprehensive understanding of the overall trend, participants must walk in a straight line for more than 10 m. This extended distance will allow for a quantitative evaluation of the gait support function by analyzing EMG data during intermediate steps where participants are not consciously adjusting their speed.

Furthermore, when utilizing a walker for walking, the outcomes may vary depending on the weight placed on the walker. During the measurement process, participants were instructed on the specific weight to be applied to the walker, practiced walking with it, and attempted to maintain consistency. However, in this experiment, we could not ensure that the weight applied to the walker remained constant during measurements. In the future, the unique characteristics of the walker should be considered and a standardized experimental environment should be established for all participants in future experiments.

Finally, participants should be unaware of the level of assistance for each trial to prevent bias in experiment results. Double-blind experiments are imperative for assessing the impact of power levels on muscle loads and the subjective appropriateness of the assistance.

4.5 Performance Evaluation of the Proposed Support Quantity

An experiment was conducted to ascertain whether the control algorithm for the proposed level of assistance could maintain a constant speed when several weights were positioned on the forearm support.

4.5.1 Purpose

The primary goal was to evaluate the capability of the smart walker's control system to maintain a steady pace under varying load conditions on the forearm support, considering that the force exerted by users on the walker can fluctuate based on factors, such as posture. In this experiment, a constant load was assumed, and tests were conducted under different load conditions to simulate real-world scenarios and assess the control system's robustness and adaptability. The experiment was designed to assess the control algorithm's ability to effectively respond to changes in force applied to the smart walker and uphold the desired speed. Additionally, to comprehensively evaluate the performance of the control system in real-world scenarios, we analyzed system responsiveness and stability under various load conditions. The objective was to identify the optimal control method to assist elderly individuals with walking.

4.5.2 Experimental Setup

The experimental setup was designed to closely mimic actual usage conditions. We utilized two speed settings based on data from a medium-scale walking experiment conducted by Hao et al. [74]. The average walking speed for elderly individuals who regularly use walkers was 0.46 m/s, whereas those who do not use walkers had an average speed of 0.79 m/s. To replicate different load conditions, weights of varying masses were added to the forearm support of the smart walker, with trials conducted at three different weight levels. For a user weighing 65 kg, the maximum load was set at approximately 20 kg, which represents approximately 30% of the user's body weight. The loaded weights were set at three levels: 8, 14, and 20 kg, with experiments conducted for each weight condition. Recognizing the possibility of variations in user weight during actual use, a propulsive force is generated from walking on the floor and the soles of the feet. Consequently, the load weight of 20 kg was chosen to ensure that the proposed algorithm could maintain walking speed even if the user significantly depended on the walker for support. The load weight of 20 kg is based on the assumption that the user will rely solely on the forearms of the walker for support, without utilizing their legs for propulsion. With a rolling friction coefficient of approximately 0.054, a load weight of 14 kg simulates the scenario where the user applies their weight to the forearm support of the walker and exerts a forward force of approximately 3.17 N, as per Equation (1). Similarly, a load weight of 8 kg replicated the situation in which the user added their body weight to the forearm support of the walker and applied a forward force of approximately 6.34 N. This method allowed for the simulation of user propulsion force variation by increasing the rolling friction force acting on the wheels and generating a force opposite to the direction of propulsion. The experiments were conducted on a 12 m straight course set up on a flat indoor floor, with a 1 m buffer zone at the end of the course to eliminate deceleration effects and focus on performance evaluation during acceleration and steady-state conditions. For the purpose of data collection, the values utilized for the input, output, and control variables were simultaneously recorded to ensure the proper functioning of the PID control. Instantaneous speed data from Hall sensors, PWM duty ratios adjusted by PID control, and self-localization data from stereo cameras were collected for detailed observation of system behavior. The analysis results were presented in graph format to facilitate an intuitive understanding of the system's behavior under each load condition.

4.5.3 Results

This section presents the findings of the performance evaluation experiment conducted on the proposed support amount determination algorithm. The purpose of the experiment was to assess the algorithm's ability to maintain speed under varying load conditions. The smart walker was equipped with a Hall sensor on each of the left and right BLDC motors. However, owing to the absence of a notable discrepancy in the recorded values of the two sensors, the data obtained from the Hall sensor on the right tire were deemed sufficient for analysis. Five trials were conducted for each parameter setting; however, no significant differences were observed between the trials. Therefore, one representative result was presented per parameter. The measured values of the sensor and actuator under varying parameter settings are shown in Figures 4.8–4.13. The vertical axes of these graphs represent the speed calculated by the Hall sensor, speed calculated from the stereo camera's self-position estimation, and PWM duty ratio adjusted by the control algorithm. The horizontal axes represent the elapsed time, with 0 representing the instant of torque generation in the motor. As evidenced in the results shown in Figures 4.8–4.10, where the target speed was set to 0.46 m/s, the speed was maintained at the target value without substantial vibration after the acceleration phase. However, instances of overshooting, defined as a temporary exceedance of the target speed, were observed during the acceleration phase. The most significant degree of overshooting was observed in conjunction with the lowest load and speed (Figure 4.8). However, the maximum speed did not exceed 1.5 times the target speed. The effectiveness of the algorithm in maintaining the target speed of 0.79 m/s is shown in Figures 4.11–4.13. Notably, the duty ratio reached its peak value of 62.75% during acceleration, regardless of the load, when targeting a speed of 0.79 m/s. Additionally, the speed calculated from the Hall sen-

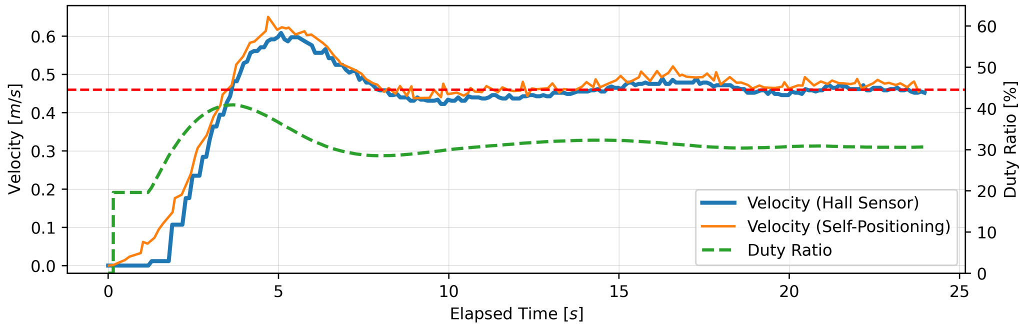

Figure 4.8: Output of the speed and duty ratio at a load capacity of 8 kg and a target speed of 0.46 m/s.

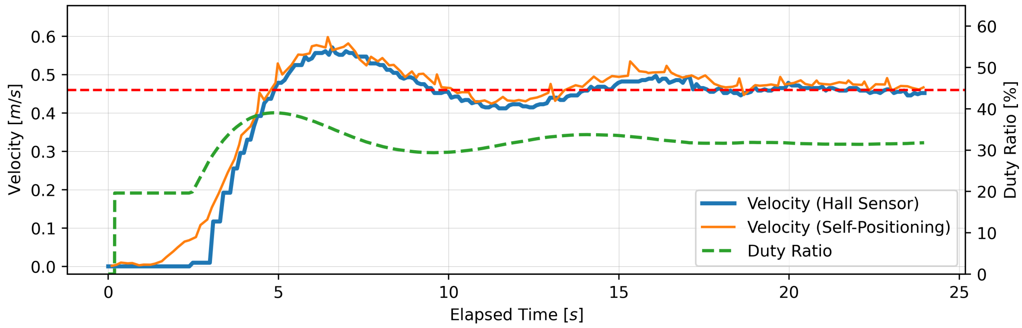

Figure 4.9: Output of the speed and duty ratio at a load capacity of 14 kg and a target speed of 0.46 m/s.

sor experienced a delay of approximately 2 s compared with that calculated from the self-position estimation. Moreover, the maximum value of the duty ratio varied under different conditions, indicating that the torque required to maintain a constant speed increased with the load. These results highlight the capability of our proposed assistance amount determination algorithm to stabilize speed despite load fluctuations. Additionally, insights were gained regarding the response characteristics of the control system under varying load conditions and the measurement characteristics of the sensor.

4.5.4 Discussion

The results of the experiments conducted on the load-dependent support level determination algorithm, as outlined in Section 4.5.3, demonstrate that the control system of the smart walker possesses the capability to maintain an optimal speed. This characteristic was adaptable regardless of the degree to which the walker bore

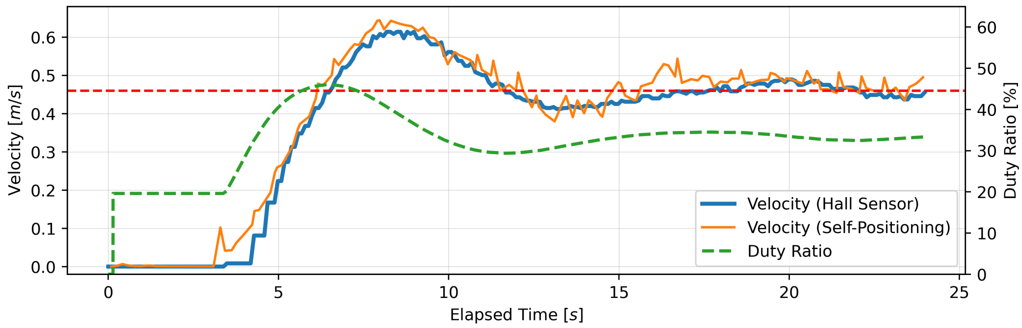

Figure 4.10: Output of the speed and duty ratio at a load capacity of 20 kg and a target speed of 0.46 m/s.

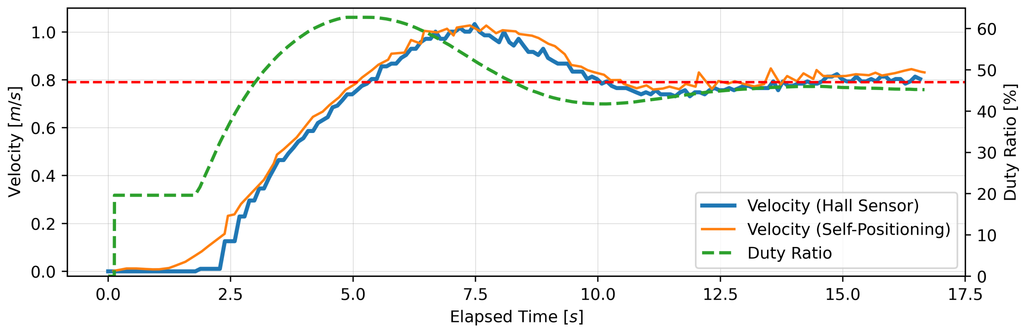

Figure 4.11: Output of the speed and duty ratio at a load capacity of 8 kg and a target speed of 0.79 m/s.

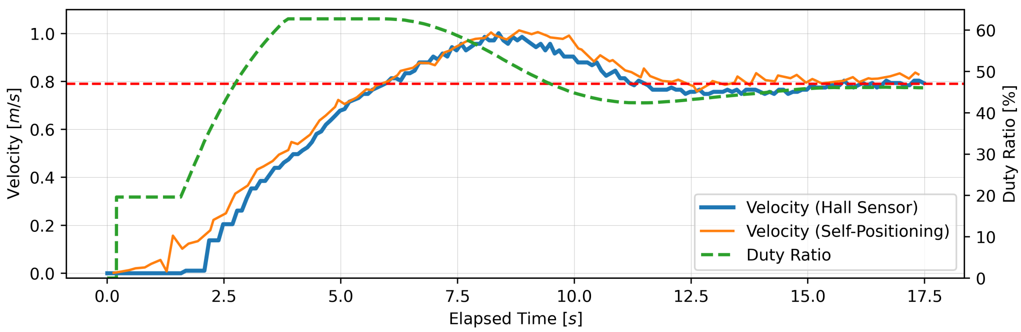

Figure 4.12: Output of the speed and duty ratio at a load capacity of 14 kg and a target speed of 0.79 m/s.

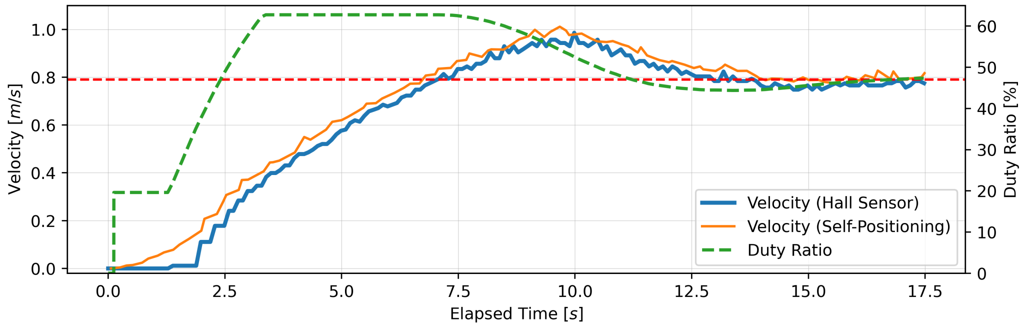

Figure 4.13: Output of speed and duty ratio at a load capacity of 20 kg and a target speed of 0.79 m/s.

the user's body weight. Such findings mark a significant stride toward the development of a walking support system that can effectively cater to the diverse needs of users. Conversely, the overshoot observed during acceleration underscored the inherent trade-off between the control system's responsiveness and stability. Through manual tuning of PID parameters, adjustments were made to align the rise time with the acceleration time during real-world walking, while considerably minimizing excessive speed resulting from overshoot. While the actual walking speed data can be approximated by appropriately adjusting the PID control parameters when the load is fixed, maintaining this approximation for varying loads proves challenging with the sensors utilized in this experiment. One contributing factor to this challenge is the variation in inertia moment and torque requirements for acceleration based on the load. To address these issues, employing a weight sensor to measure the load on the smart walker and dynamically adjusting the PID control parameters in response to the weight is recommended. Additionally, enhancing the performance of the computing devices utilized is crucial to reducing response delays. When transitioning to different devices, a detailed analysis of the processes causing time bottlenecks in determining the support level is essential for optimization. The delay in the Hall sensor measurements (approximately 2 s) clearly demonstrated the challenge of speed control in the low-speed range. This delay poses a significant obstacle when attempting to accelerate and gain propulsion. To address this issue, the integration of sensor fusion technology should be explored, which combines data from the stereo camera and Hall sensor, or the implementation of more sensitive sensors. The observed increase in torque requirements resulting from an increase in load is a crucial finding that showcases the adaptability of the control system. By ensuring the ability to maintain speed under varying load conditions, we can tailor the system to satisfy the unique needs of each user and their environment, providing more personalized and advanced support.

4.6 Walking Experiment Utilizing the Proposed Support Amount Algorithm

The objective of the proposed support amount control algorithm is to ensure that the robot aligns its support with the user's walking intention. Accordingly, walking experiments will be conducted to validate that the algorithm does not deviate from the user's intended walking pattern when utilizing the smart walker.

4.6.1 Purpose

The principal objective of this experiment is to assess the practicality and safety of the proposed control algorithm, specifically in ascertaining whether the physical strain on the user can be reduced user while maintaining their natural gait when utilizing a walker. The impact of enhancing the user's mobility, a primary objective of smart walkers, is challenging to quantify owing to its subjective nature. Moreover, the optimal level of assistance varies depending on the individual's unique walking patterns. In previous studies, electromyography has been utilized occasionally. However, as noted by Cram [75], this approach is associated with several challenges, including the difficulty of accurately positioning electrodes and the complexity of interpreting the resulting data, as highlighted by Disselhorst-Klug et al. [76]. In view of these considerations, this study focuses on utilizing more generalizable evaluation metrics, such as irregular changes in speed and excessive load in relation to the user's intention. This approach allows for an objective and comprehensive evaluation that is less influenced by individual differences and subjective factors. In particular, we employed an analytical approach that integrates data from measurements with responses from questionnaires completed by the participants. This method allows for a comprehensive evaluation of the system's stability and safety during walking.

4.6.2 Experimental Setup and Procedure

To validate the algorithmic output's reliability concerning assistance and ambulatory stability, this experiment involved five participants in their twenties with a low risk of falling and no history of lower limb issues. Prior to the commencement of the experiment, the participants received detailed information regarding the research purpose, potential risks, and the requirements of informed consent, in accordance with the guidelines outlined in the Declaration of Helsinki. The participants then provided their consent to participate in the experiment. Furthermore, the questionnaire items listed in Table 4.2 were elucidated before the experiment. Because the participants were younger than the intended users, a 10 kg vest-type weight and 1 kg weight on each ankle were added to increase the walking load, aiming to replicate the walking conditions of elderly or mobility-impaired individuals more accurately. The experimental procedure was as follows:

1. Participants were provided with an explanation of the operational principles of the walker, followed by a minimum of 5 mins of unstructured walking time to familiarize themselves with the device.

2. The steady walking speed of each participant was measured and established as their individual target speed. This measurement was based on the average speed of the central portion (4 s) between the acceleration start and stop as the target speed for the 12 m straight course. The same measurement method was employed to determine the target speeds for the left and right motors on the circular course.

3. The walker, equipped with the proposed control algorithm, was utilized to navigate two distinct types of courses.

    (a) 12 m straight course (six trials)

    (b) Circular course with a radius of 2 m, two laps (three trials)

Data recorded during each trial included walking speed calculated from self-position estimation by the stereo camera, speed obtained from BLDC motor hall sensors, and PWM duty ratio. These measurements were utilized to validate the absence of unintended fluctuations in speed and that the duty ratio did not exhibit excessive numerical fluctuations (defined as vibrations of 5% or more per second).

Table 4.2: Questions to subjects after all trials.

No.	Question
Q1	During straight forward walking, I felt assistance in the same direction as my intended movement
Q2	During straight forward walking, variations in the amount of assistance did not interfere with my normal walking
Q3	During circular course walking, I felt assistance in the same direction as my intended movement
Q4	During circular course walking, variations in the amount of assistance did not interfere with my normal turning motion

Upon completion of all courses, participants were asked to complete a questionnaire based on the items outlined in Table 4.2. Additionally, participants were encouraged to provide free-form opinions for each trial. This experimental design aimed to assess the practicality and safety of the proposed algorithm, as well as to gain valuable insights for future clinical applications.

4.6.3 Experimental Results

The objective of this section is to elucidate, through a subject experiment, that the control algorithm for the level of support, as designed in Section 4.3, can maintain a steady state speed with no additional load on the actual user's walking. The results of the measurement of each participant's walking speed in a steady state are shown in Table 4.3. The steady state was defined as the speed during the middle part (4 s) of the period from the start of acceleration to the stop, focusing on the section with minimal variation in walking speed. The average walking speed of the participants in this experiment was within the speed range (0.46 –0.79 m/s) assumed in the experiment using the weights in Section 4.5.2.

The results of the 12 m straight-line walking experiment demonstrated three primary trends in the relationship between speed variation and duty ratio. Figures 4.15–4.17 illustrate representative patterns of these. The vertical axis of each graph depicts the speed as measured by the Hall sensor, the speed as estimated by the stereo camera, and the PWM duty ratio, while the horizontal axis represents the elapsed time

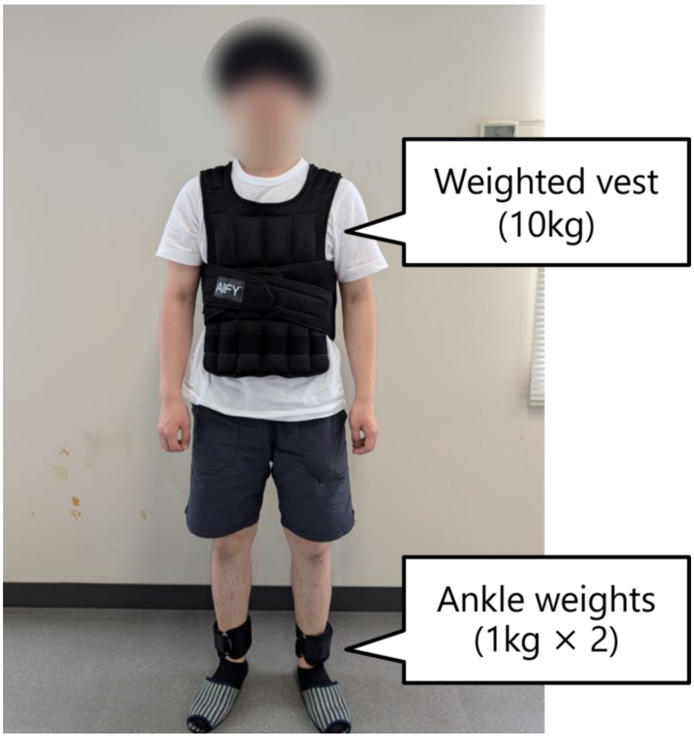

Figure 4.14: Subject with weights attached.

Table 4.3: Statistics on walking speed when using a walker in the absence of support..

Subject Labels	Mean	SD	Min	Max
Subject A	0.601	0.034	0.538	0.657
Subject B	0.741	0.025	0.692	0.780
Subject C	0.629	0.015	0.603	0.668
Subject D	0.754	0.023	0.711	0.809
Subject E	0.656	0.028	0.597	0.704

from the point at which the motor torque was generated. Figure 4.15 (Subject A) illustrates a pattern wherein the speed stabilized at the target speed, concomitant with a stabilization of the duty ratio. Figure 4.16 (Subject C) depicts a scenario wherein the walking speed surpassed the pre-established steady-state speed, accompanied by a discernible tendency for the motor torque to decline gradually. Figure 4.17 (Subject E) illustrates a gradual increase in torque at the commencement of walking, followed by a phenomenon of the motor reaching maximum torque and subsequently decelerating to achieve the ideal walking speed. In all the trials conducted with all the subjects, there were no significant deviations from the intended route, and no sudden

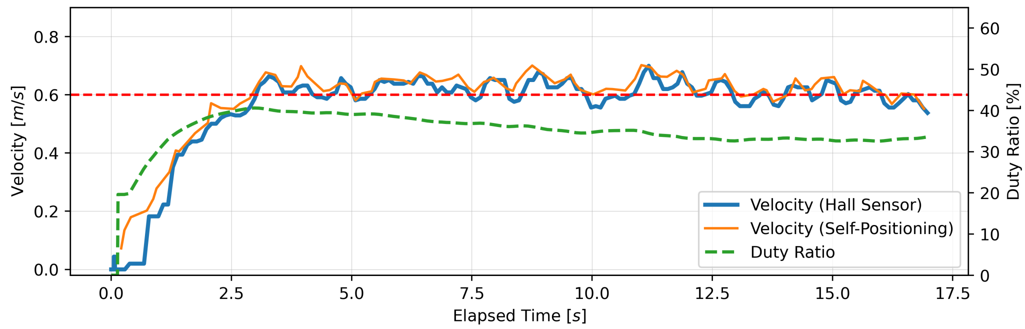

Figure 4.15: Single trial where walking speed stabilized at the target walking speed. The red dotted line represents Subject A's average normal walking speed (0.601 m/s).

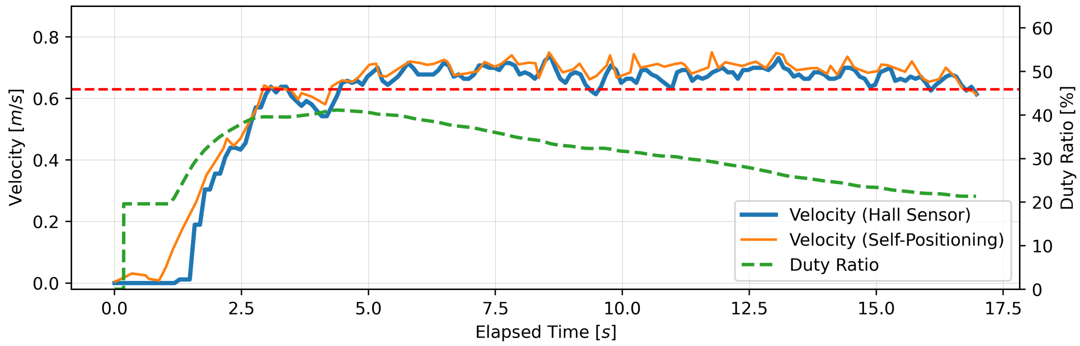

Figure 4.16: Trial where walking speed stabilized above the target speed. The red dotted line represents Subject C's average normal walking speed (0.629 m/s).

acceleration or dangerous changes in speed were observed. In each subject's trial, a consistent tendency was observed whereby the walking speed stabilized around the target speed.

The results for the two-lap course with a two-meter radius exhibited a comparable pattern to that observed in straight-ahead walking. The results for the lap route will be presented as representative examples. Figure 4.18 illustrates the speed change and duty ratio for a single trial conducted by Subject C. The vertical axis of the graph depicts the speed measured by the left and right Hall sensors and the PWM duty ratio, while the horizontal axis represents the elapsed time from the point at which the motor torque was generated. In the case of Subject C, the optimal speed for a 2 m radius was found to be 0.504 m/s for the left tire and 0.714 m/s for the right tire. The experimental results demonstrated that these specific speeds were generally maintained during walking.

A questionnaire was employed to ascertain whether any load could not be observed

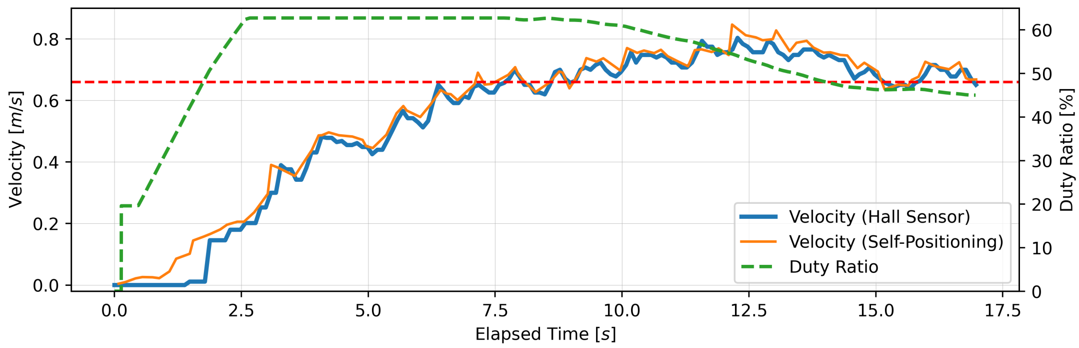

Figure 4.17: Trial with a slow initial speed. The red dotted line represents Subject E's average normal walking speed (0.656 m/s).

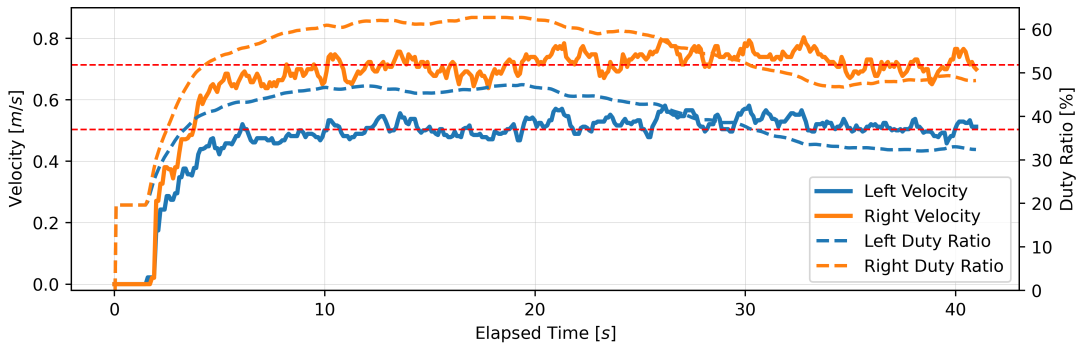

Figure 4.18: Trial of the circular route. Based on the pre-measurement results of Subject C, the ideal velocity for the left wheel was calculated to be 0.504 m/s, and for the right wheel 0.714 m/s.

by the sensors installed in the smart walker. This was conducted after all the trials had been completed. The results of the subjects' answers to the questions in Table 4.2 are presented in Table 4.4. For Q1, four subjects answered "Totally Agree" and one answered "Agree". For Q2, three subjects answered "Totally Agree" and two answered "Agree". For Q3, three subjects answered "Totally Agree", one answered "Agree", and one answered "Neutral". For Q4, three subjects answered "Totally Agree" and two answered "Agree". The following responses were obtained from the open-ended questions about overall support and each trial.

- I felt the force in an unintended direction only once when walking on the circular course in one trial (Subject A);
- I did not feel much support when walking on the circular course (Subject B);

Table 4.4: Subjects' answers to the questions in Table 4.2..

Subject Labels	Q1	Q2	Q3	Q4
Subject A	Totally Agree	Totally Agree	Agree	Totally Agree
Subject B	Agree	Totally Agree	Neutral	Agree
Subject C	Totally Agree	Agree	Totally Agree	Totally Agree
Subject D	Totally Agree	Totally Agree	Totally Agree	Totally Agree
Subject E	Totally Agree	Agree	Totally Agree	Agree

- I felt that it would be okay to increase the amount of support even a little when walking in a straight line (Subject B);
- I felt the motor fluctuate depending on the speed, but it was not a change where the walker suddenly pulled me (Subject C);
- It was difficult to tell whether it was getting easier or not (Subject C);
- I felt that the strength of the motor was appropriate (Subject D);
- I felt that the walker was moving forward (Subject E).

4.6.4 Discussion

The efficacy and reliability of the system when utilized by users in authentic scenarios were substantiated by the experimental outcomes presented in Section 4.6.3. The primary outcome was that the algorithm exhibited consistent and reliable speed maintenance capabilities in real-world usage scenarios. Nevertheless, a number of issues were also identified. The observed differences in steady-state walking speed among the subjects indicate the diversity of individual walking characteristics. This result indicates the necessity for a control system for a smart walker that is capable of adapting flexibly to the walking patterns of individual users. It will be necessary in the future to develop an adaptive control system that learns the walking characteristics of the user and optimizes them over time. In particular, if we can identify the gait cycle using motion tracking technology, it will become possible to adjust the amount of assistance according to the cycle. Specifically, since elderly individuals tend to have a reduced ability to push off with their feet during the swing phase of walking [77], a control system that varies the amount of assistance during specific gait phases can be considered. The three types of speed-duty ratio patterns observed in the straight-line walking experiment demonstrated the adaptability and robustness of the proposed algorithm. In particular, the stabilization of speed in proximity to the target speed observed in all the subjects indicates a high degree of capability to maintain speed during the act of steady walking. However, further investigation is required to elucidate the reasons behind the deviation from the target speed observed in some trials, particularly the phenomenon observed in Figure 4.16. The observation in Figure 4.16, wherein the user maintains a slightly elevated speed relative to the target speed and exhibits no deceleration despite the reduction in torque, indicates a potential interaction between the user's gait and the algorithmic control. This phenomenon suggests that the user, who is aware of maintaining speed, may be increasing the propulsion force gradually unconsciously. To substantiate this hypothesis, a more comprehensive biomechanical analysis and prolonged walking experiments are necessary. One of the limitations of this study is that it was not feasible to continue walking until the torque stabilized completely due to the restricted length of the experiment (12 m). Potential solutions to this issue include conducting longer walking experiments and long-term observation of steady-state walking using a treadmill. Conversely, enhancing the responsiveness of speed adjustment by expanding the scope of torque fluctuations is a potential avenue for improvement. However, there is a risk that abrupt alterations in the level of support may have a detrimental impact on the user's posture control or, alternatively, may result in a reduction in the capacity to maintain speed. The optimization of this trade-off represents a significant research opportunity for the future. Another limitation of the algorithm is its inability to adapt to situations where the user's target walking speed changes. For example, when walking while conversing with another person, the user needs to match the walking speed of their companion. As a result, the target speed differs from the user's usual ideal walking speed. In such cases, the current algorithm cannot accommodate these variations. From the perspective of safety, it is noteworthy that no sudden acceleration or dangerous changes in speed were observed throughout all the trials. In addition, the proposed support amount determination algorithm did not fluctuate the support amount suddenly, and it did not affect the user's walking posture. The results demonstrate that the proposed algorithm is capable of providing effective support while ensuring the safety of walking. Nevertheless, it is imperative to conduct further verification and establish this safety through long-term clinical trials with actual elderly individuals and those with heavy walking loads. In this validation, to confirm that the proposed algorithm can track the subjects' target speeds, we conducted tests on five individuals with a low risk of falling during walking. To approximate the walking conditions of the intended users, measurements were taken under increased walking load by attaching additional weights. Ensuring safety in real-world environments will require a larger and more diverse sample, including elderly individuals and those with mild motor impairments. In addition, in the parameter adjustment for this study, it was confirmed from Figures 4.8–4.13 that there is no steady-state error for short-term walking of less than 12 m. However, since incremental PID control is employed, there is a possibility that an integral truncation effect may occur. Therefore, additional verification regarding the accumulation of long-term errors is necessary.

4.7 Conclusion

Chapter 4 presents the results of research on the implementation of support functions to assist with propulsion force in smart walkers. The propulsion force assistance function was crucial when the propulsion force generated by the user's voluntary walking could not achieve the target speed. In this study, a propulsion force assistance function based on speed-type PID control was proposed to achieve the target speed required for safe walking in a nursing care facility.

To assess the impact of motor torque assistance on reducing the physical strain of walking in a forearm-supported walker, an evaluation experiment was conducted with participants. The evaluation methods included a questionnaire survey as a subjective indicator and surface electromyography to measure maximum voluntary muscle strength as an objective indicator, and quantitatively analyzed changes in lower limb muscle activity. The results of the experiment indicated that utilizing motor torque to assist propulsion in a forearm-supported walker effectively reduced the load on the legs during short-term walking and contributed to changes in the amount of muscle activity in the lower limbs. Furthermore, performance evaluations of the proposed dynamic propulsion assistance function demonstrated excellent speed tracking performance and no impediments to walking owing to the propulsion assistance, as validated through experiments in a simulated environment with added weights and trials with participants.

Moving forward, a key area for future research involves understanding how to gauge user behavioral intention when the target speed fluctuates during walking, such as when walking alongside others or when decelerating.

Chapter 5

Obstacle Avoidance Using Depth Images

5.1 Introduction

In an aging society, the need for assistive devices that promote independent living among the elderly has increased. One critical aspect of this is ensuring the safety of walking assistance devices, as preventing falls and collisions is a top priority. These incidents can result in serious injuries, such as fractures, and can often lead to individuals becoming bedridden. Traditionally, manual walking assistance involves skilled caregivers who monitor the environment, guide users along safe paths, and assess distances from obstacles. The incorporation of these safety assurance functions of human assistance in smart walkers is crucial.

Simply implementing emergency stop functions is not sufficient to guarantee the safety of walking assistance devices. Users may intentionally approach objects, making overly sensitive emergency stop features impractical for daily use. Therefore, the demand for obstacle avoidance systems that can adapt to the user's intentions and surroundings, ensuring a more flexible and user-friendly experience has increased.

Stereo camera systems offer numerous advantages when selecting environmental recognition sensors. They provide high spatial resolution for thorough knowledge, allowing for a detailed understanding of obstacle shapes and positions of obstacle shapes and positions. Additionally, when combined with image recognition technology, they enable object classification. Not only do stereo camera systems offer these benefits, but they are less costly compared with laser sensors and LiDAR, while consuming relatively less power. These advantages contribute to achieving space efficiency and extended operation time in battery-powered smart walkers. Recent advancements in image processing technology have further improved the reliability and processing speed of stereo camera systems.

This study proposes an obstacle direction detection and avoidance system that utilizes depth images obtained from stereo cameras. This system identifies the position of the nearest object using real-time depth information and selects appropriate actions based on relative position and approach velocity. In particular, the system performs emergency stops for frontal object approaches and executes gentle avoidance maneuvers in safe directions for approaches from the left or right front. The effectiveness of the proposed method will be validated empirically through multiple experimental scenarios in real environments, particularly through collision prevention experiments with walls and moving objects. The goal is to develop a new walking assistance system that prioritizes safety and usability while supporting independent mobility for walker users.

The remainder of this section is organized as follows. Section 5.2 outlines the purpose and methodology of the obstacle avoidance function. Section 5.3 details the experiment conducted to evaluate the obstacle direction estimation. Section 5.4 presents the experiment on collision scenarios with walls to assess the effectiveness of obstacle avoidance based on the evaluation value determined in Section 5.3. Section 5.5 summarizes this chapter.

5.2 Obstacle Avoidance Algorithm

5.2.1 Purpose

There are two types of objects that a walker may collide with in a nursing home. Static objects, such as walls and beds, and dynamic objects, such as caregivers and wheelchairs in use. For static objects, avoidance action can be determined by checking the positional relationship between the walker and the static object in advance. For dynamic objects, the avoidance action needs to be determined just before contact is made, or the obstacle trajectory prediction method [78, 79] should be used to determine the avoidance action. This thesis deals with obstacle avoidance for static objects that can serve as the basis.

Collision avoidance with obstacles is performed by two actions: emergency stop and avoidance by directional control. Most conventional smart walkers perform obstacle avoidance by emergency stop. However, stopping each time an obstacle appears requires repeated acceleration and deceleration during walking, which can be burdensome for the user. Additionally, when moving straight ahead at shallow angle to a corridor wall, it is more natural for the user to change direction so that he or she is parallel to or away from the direction of the wall, rather than making an emergency stop. Therefore, avoidance is performed by directional control of the walker using depth images from a stereo camera and motor control in such cases.

5.2.2 Approach

To achieve the above purposes, one of the following three obstacle avoidance actions must be selected.

- Emergency stop
- Turn left while decelerating
- Turn right while decelerating

To determine these actions, the positional relationship between the walker and the obstacle must be known. Then the actual motorized obstacle avoidance is performed. These are shown separately in the obstacle direction estimation module and the obstacle avoidance module.

Obstacle Direction Estimation Module

For obstacle avoidance, if there is an obstacle ahead, an emergency stop is performed; if there is an obstacle on the front left, a right turn is performed while decelerating; and if there is an obstacle on the front right, a left turn is performed while decelerating. Therefore, there are three outputs of the obstacle direction estimation algorithm: forward, right forward, left forward. The following describes the depth image that is the input to the obstacle direction estimation algorithm. Three areas are defined in the depth image. Figure 5.1 shows the three areas in the depth image acquired. The first is the center area, which is used to determine whether or not obstacle avoidance is necessary. The area in the center is defined as $area_c$. $area_c$ is located at $0 - 3/5$

up and down, and 2/5 – 3/5 left and right: a3, a8 and a13 in Figure 5.1. The second is the left area, which is used to determine if an obstacle is in the front left side. The area in the left is defined as $area_l$. $area_l$ is located 2/5 – 3/5 up and down and 0 – 2/5 left: a11 and a12 in Figure 5.1. The third is the right area, which determines whether the obstacle is in the front right side or not. The area in the right is defined as $area_r$. $area_r$ is located 2/5 – 3/5 up and down, and 3/5 – 5/5 right: a14 and a15 in Figure 5.1. Because there are many variations in the values to be determined for these areas, they were determined after checking the depth images of various situations. The reason for omitting the lower area is that the distance to the floor surface reflected in the camera is approximately 1.0 m, which affects the minimum distance. There are also two possible values to use as thresholds: the minimum and average values in the area. The advantage of using the minimum value within a region is that it requires less computation and leads to the identification of the specific location of the obstacle. The advantage of using the average value in the areas is that it reduces the influence of specific noise pixels. These two evaluation values are validated in the experiments in Section 5.3 as comparison items. If the ratio of these left/right evaluation values exceeds a set threshold, the obstacle is determined to be on either side, and if the ratio does not exceed the threshold, the obstacle is determined to be in the center. Algorithm 1 is a concise summary of these.

The procedure of the obstacle direction estimation module is shown below. First, the depth image is subjected to appropriate preprocessing. An overview of the preprocessing is shown in Figure 5.2. The left edge of the depth image is sliced off by 30 pixels. This is done to offset the fact that the image is shifted from the center of the camera because the depth distance is calculated based on the information of one camera using the information of the other camera as a feature of the depth image generation by the stereo camera. Because the distance in $area_c$ is used to determine the distance, the left side of the image must be partially cropped to align the center position of the camera with the center position of the depth image. In depth estimation methods using stereo cameras, there are pixels for which depth cannot be measured. For example, areas that are in a blind spot from the camera used for depth calculations or degraded images due to camera shake are regarded as unmeasurable. If the pixel with x-axis i and y-axis j is measurable, then $MP_{ij} = 0$. If it is not measurable, $MP_{ij} = 1$. When calculating the evaluation value of direction

Algorithm 1 Estimated obstacle direction

Require: $dist_l$: Evaluated value in $area_l$

Require: $dist_r$: Evaluated value in $area_r$

Require: th: Threshold for the center direction

Ensure: $direction$: Obstacle direction (0: left, 1: center, 2: right)

$dicrection \leftarrow 0$
if $dist_l < dist_r$ **then**
    $ratio \leftarrow dist_r/dist_l$
    if $ratio \leq th$ **then**
        $direction \leftarrow 1$
    else
        $direction \leftarrow 0$
    end if
else
    $ratio \leftarrow dist_l/dist_r$
    if $ratio \leq th$ **then**
        $direction \leftarrow 1$
    else
        $direction \leftarrow 2$
    end if
end if

estimation, pixels with $MP_{ij} = 1$ are excluded from the calculation. if $area_l$, $area_l$, or $area_r$ are all pixels with $MP = 1$, an emergency stop is performed.

Obstacle Avoidance Module

In case of an emergency stop, both brushless DC motors apply the brakes. If there is an obstacle to the right, the left brushless DC motor applies the brake to turn the walker to the left. If there is an obstacle in the left direction, the right brushless DC motor will apply the brake in order to turn the walker to the right. The amount of brake torque is determined in Section 5.3.1.

The distance of the warning area is explained. If the minimum distance falls

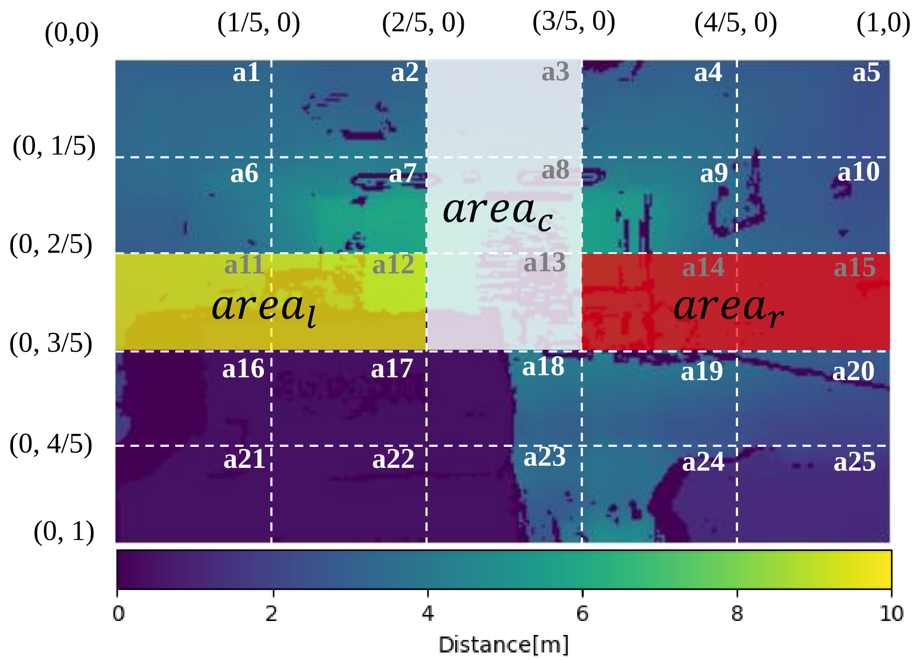

Figure 5.1: Areas used for obstacle direction estimation.

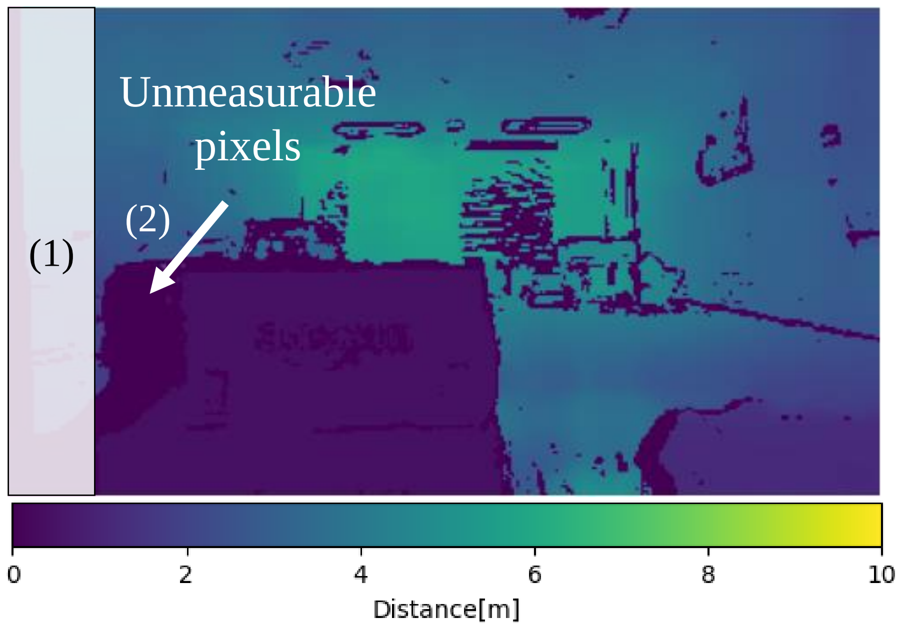

Figure 5.2: Depth image preprocessing. (1) Delete to align the center position of the camera with the center position of the depth image. (2) Exclude unmeasurable pixels from the calculation of evaluation values.

Table 5.1: Relation between speed of the walker and the distance to the avoidance processing.

Speed of the walker [m/s]	Distance to the avoidance processing [m]
≤ 0.3	0.6
≤ 0.4	0.7
≤ 0.5	0.8
≤ 0.6	0.9
≤ 0.7	1.0
≤ 0.8	1.2
> 0.8	1.4

below a certain threshold, it means that an object exists in the warning area, and this distance is defined as the warning area distance. The distance of the warning area varies depending on the speed of the walker. The reason for this is that the damage to the user in the event of a collision is different when approaching a wall slowly and when approaching a wall quickly. Moreover, when approaching a wall or an installation slowly, the user often does not intend to make contact with the wall or installation, but to move closer to it. This mechanism of changing the warning area with the speed of the walker is also used in the AGoRA Walker [80]. The relationship between the amount of stopping torque and the braking distance at the speed of the walker was obtained from preliminary experiments, and the relationship between the speed of the walker and the shortest distance in the central area to the warning area was defined as presented in Table 5.1.

5.3 Experiments on the Evaluation Values Used in the Direction Estimation Algorithm

5.3.1 Experimental Setup

Three types of collisions with flat surfaces and three with obstacles were measured. The plane collisions were measured for collisions perpendicular to the wall surface and for collisions at 45° angles to the wall surface. For collisions with obstacles, the cases where the walker was facing the obstacle and collided with it head-on and the

Table 5.2: Number of depth images used in the experiment.

	left	cetner	right	None
Wall	260	284	210	-
Obstacle	234	254	244	228

cases where the walker was facing the obstacle and collided only with one side of the obstacle were measured. These measurements were made using an actual walker, and depth images were acquired by moving the walker back and forth between 0.3 and 2.5 meters. The number of depth images when limited to only 1.4 m or less, which is the shortest distance for actual avoidance behavior, is presented in Table 5.2. These depth images were used with the minimum and average values. These are the evaluation values specified in Section 5.2.2, to determine whether the algorithm identifies an obstacle in either direction. The threshold values were determined from 1.05 to 1.3 in increments of 0.05.

5.3.2 Results

The results of the minimum and mean evaluated value are listed in Table 5.3. The threshold value th for determining the center is described from 1.05 to 1.3 in increments of 0.05.

When the evaluated value was set to the minimum value, a high accuracy of approximately 95% was confirmed when the object approached the wall at 45 ° to the left and right. Although a larger value of t increases the number of images determined to be centered, an accuracy of approximately 84% was confirmed even at the maximum value of 1.3, which is the threshold set. The results for the case of a vertical straight walk to the wall differed depending on the threshold value. At the minimum threshold value of 1.05, the accuracy rate was approximately 50%, and it increased to approximately 85% when the threshold value was increased to 1.3. When the vehicle moved forward vertically to the obstacle, the rate was approximately 37%, regardless of the threshold value.

When the evaluation value was set to the average value, the result against the wall was not much different from the result with the minimum evaluation value. However, in the case of a collision to the left of an obstacle, the correct response rate was

Table 5.3: Estimation results using the minimum and mean.

evaluation value	threshold for ratio	Wall left	Wall center	Wall right	Obstacle left	Obstacle center	Obstacle right
minimum	1.05	0.969	0.5	1.0	0.9915	0.370	1.0
	1.1	0.954	0.739	1.0	0.992	0.370	1.0
	1.15	0.946	0.806	1.0	0.992	0.370	0.980
	1.2	0.939	0.831	1.0	0.992	0.370	0.926
	1.25	0.939	0.845	1.0	0.987	0.370	0.836
	1.3	0.935	0.849	1.0	0.987	0.374	0.791
mean	1.05	1.0	0.559	0.995	0.992	0.130	0.266
	1.1	1.0	0.801	0.995	0.979	0.252	0.189
	1.15	1.0	0.843	0.995	0.936	0.386	0.160
	1.2	1.0	0.853	0.991	0.633	0.539	0.111
	1.25	1.0	0.853	0.991	0.329	0.705	0.041
	1.3	0.996	0.853	0.991	0.209	0.976	0.016

approximately 99% for a threshold of 1.05, but dropped to approximately 21% for a threshold of 1.3. In the case of moving straight towards the obstacle, the correct response rate was approximately 13% at the 1.05 threshold but increased to 97% when the threshold was increased to 1.3. However, for collisions to the right of the obstacle, the response rate was less than 26% regardless of the threshold value.

5.3.3 Discussion and Threshold Selection

When the minimum value was used as the evaluation value, a threshold value of 1.15 was used, which resulted in correct deductions in more than 80% of the images, except in the case of approaching obstacles perpendicularly. Moreover, in images where the left and right deductions were incorrect, the obstacle was incorrectly determined to be in the center. However, when the average value was used as the evaluation value, the estimation accuracy for the obstacles was low regardless of the threshold value used. This result is discussed in the following example of an actual image used for the estimation. Figure 5.3 shows images in which the output results differ between the minimum and average values. When the minimum value was used, the obstacle was

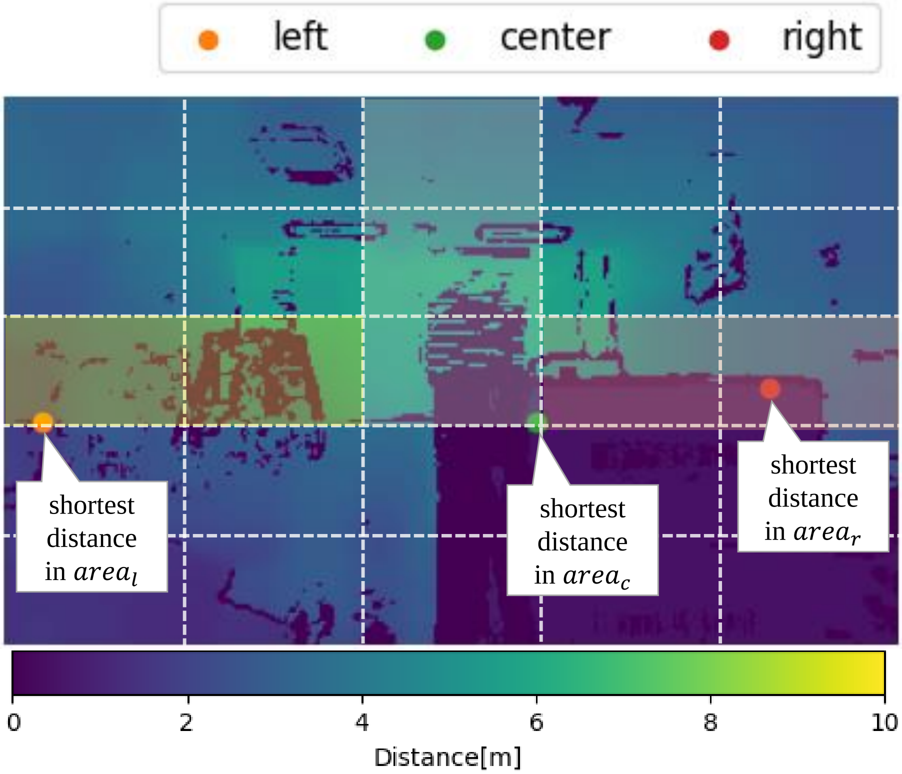

Figure 5.3: Examples of depth images with different deduction results. Actually an obstacle on the right. Using the minimum value, it is deduced to the right. Using the mean value, it is deduced to the center.

determined to be on the right, which is the correct direction, and when the average value was used, the obstacle was determined to be in the center, which is the wrong direction. This may be due to the fact that the depth of the room and other factors were added to the calculation by averaging the images. Therefore, in this case, the minimum value that can detect fixed obstacles other than walls was adopted, and the threshold value was determined to be 1.15, which was highly accurate.

5.4 Obstacle Avoidance Experiment Against Walls

5.4.1 Purpose

The experiment clarified whether the three types of avoidance actions set in Section 5.2.2 and the threshold th determined in Section 5.3 can correctly avoid a wall or not. The trajectory of the walker is clarified from the results of the walker's self-position estimation and the relationship graph between the distance and velocity in the depth image.

5.4.2 Experimental Setup

The experiment was conducted with three subjects in their 20s with no history of foot-related problems. To prevent the subjects from intentionally avoiding obstacles, they were asked to use the walker by placing their arms on the support part of the walker without touching the handrails. The subjects performed three types of walking, walking straight ahead from a distance of 3.5 m from the wall at an angle of 45 ° to the front and to the left and right. Six trials were performed in each of the three directions.

The following settings were made for the amount of stopping torque: In the case of an emergency stop, stopping torque is applied to both motors. For a right turn, a signal is sent to the left motor to generate torque in the backward direction. Equation 5.1 is the value used to calculate the actual torque used, and the maximum amount of torque the motors can create is 255. p is the amount of torque to be generated and s is the speed of the walker.

$$p = 90 + (s^2 \times 100) \tag{5.1}$$

5.4.3 Results

Table 5.4 shows the results of direction estimation and collision avoidance for all trials for all subjects. In all the trials, the left and right avoidance was normal, and there were no trials in which the subject came into contact with the wall. However, in the case of subject B straight forward movement vertically against a wall, a collision with the wall was observed in one of the runs. This was because the direction estimation algorithm judged it to be left instead of frontal, and it turned to the right while decelerating. When the direction estimation algorithm indicated the correct direction of the obstacle, the subject was able to avoid the wall appropriately.

The results of all trials for subject A are shown. Figure 5.4 depicts the trajectory of the six trials when the subject moved straight ahead at 45 ° to the right relative to the wall surface. The vertical and horizontal axes indicate the actual position coordinates, respectively, in meters. Figure 5.5 shows the relationship between the depth image distance and speed for one of the trials in Figure 5.4. The horizontal

Table 5.4: Results of direction estimation and collision avoidance for all trials for all subjects.

Subject	Actual wall direction	Total number of trials	Number of correct direction estimations	Number of collisions
A	left	6	6	0
	center	6	6	0
	right	6	6	0
B	left	6	6	0
	center	6	5	1
	right	6	6	0
C	left	6	6	0
	center	6	6	0
	right	6	6	0

axis shows the elapsed time since the start of walking. The red vertical line indicates the time when the motor is actually signaled for the avoidance action using the depth image from the stereo camera. Figure 5.6 depicts the trajectory of six trials for a straight line perpendicular to the wall surface. Figure 5.7 shows the relationship between the depth image distance and speed for one trial in Figure 5.6. Figure 5.8 depicts the trajectory of six trials in the case of a straight line at 45 ° left to the wall surface. Figure 5.9 is a graph showing the relationship between the depth image distance and velocity for one of the trials in Figure 5.8.

5.4.4 Discussion

From Figure 5.4 and Figure 5.8, it is clear that the direction of travel is changed to avoid collision against the wall. Additionally, it can be confirmed from Figure 5.5 and Figure 5.9 that the left and right depth distances increase after avoidance (red vertical lines), indicating that the vehicle moved away from the wall that existed in front of it. These results indicate that collisions with walls can be avoided automatically in the appropriate direction without repeated emergency stops.

This experiment confirmed the feasibility of the avoidance action. However, although it should be confirmed that there is no burden on the user (e.g., the walker

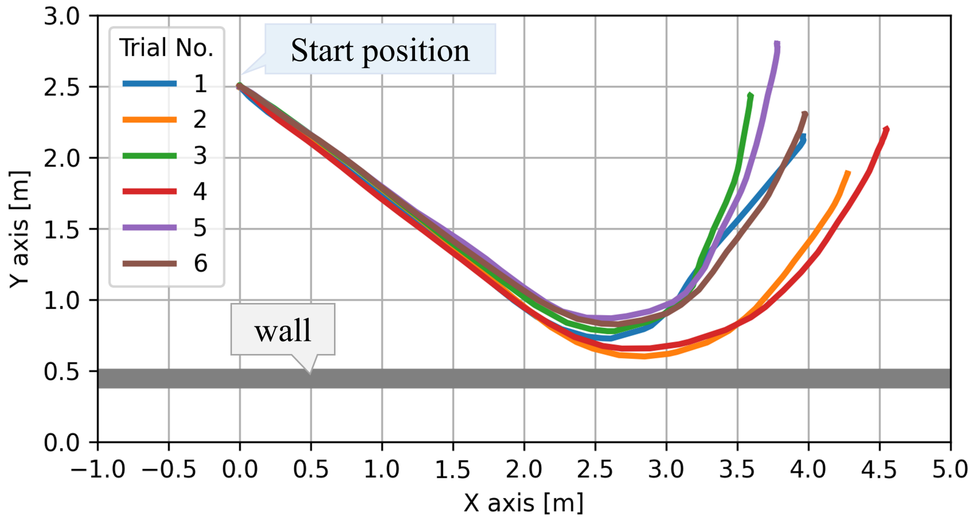

Figure 5.4: Overhead view of the trajectory for walker when moving straight ahead at 45 ° to the right relative to the wall.

forcibly changing direction) when performing the avoidance action, this was omitted from the verification items in this study. A questionnaire was sent to the subjects, and it was confirmed that there was no sensation of being pulled by the walker; however, this could be attributed to the ages of the subjects. Because the walker is used by the elderly, the burden on the user in the avoidance action could not be properly evaluated for this subject. As a future prospect, we would like to evaluate the burden of avoidance action by having elderly people, the target users, actually use this walker.

5.5 Conclusion

This section presented the findings of a study on the implementation of collision prevention functions using depth images. Accidents, such as falls resulting from collisions can lead to external injuries and are identified as a primary factor necessitating nursing care for users. To mitigate collisions while using a walker, the optimal collision avoidance direction and control intensity should be dynamically adjusted based on the forward environment and walking speed of the walker.

This research introduced an obstacle avoidance function utilizing motor control that integrated depth images derived from a stereo camera and walker speed information. The experiment involved setting obstacles, such as a wall and bed, as collision

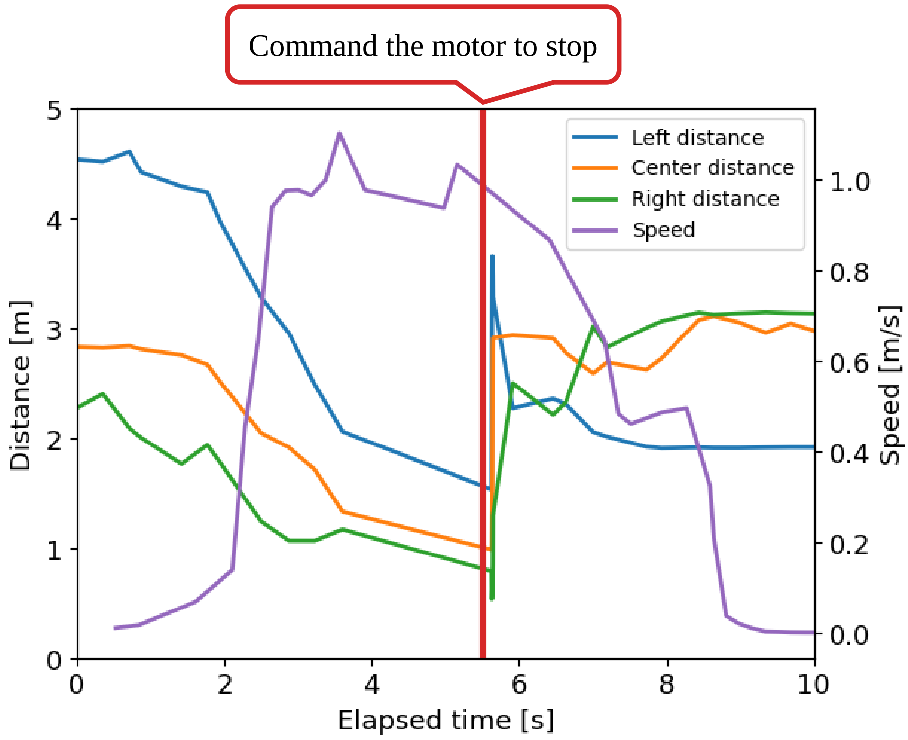

Figure 5.5: Relationship between depth image distance and velocity when walking straight ahead at 45 ° to the right relative to the wall.

avoidance targets to evaluate the estimation of obstacle direction and effectiveness of the collision avoidance function. The experimental results demonstrated the effectiveness of the collision avoidance function in a specific scenario. By analyzing the path of avoidance and the change in speed of the walker when approaching from the

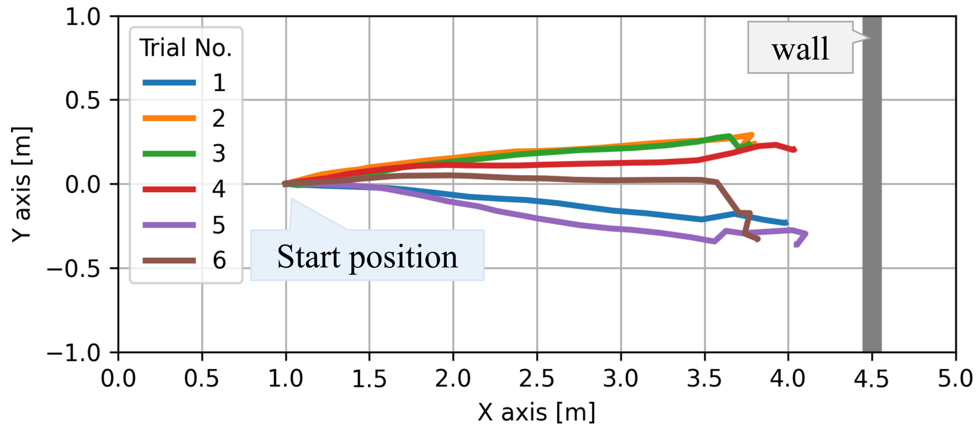

Figure 5.6: Overhead view of the trajectory for walker when walking straight ahead vertically to the wall.

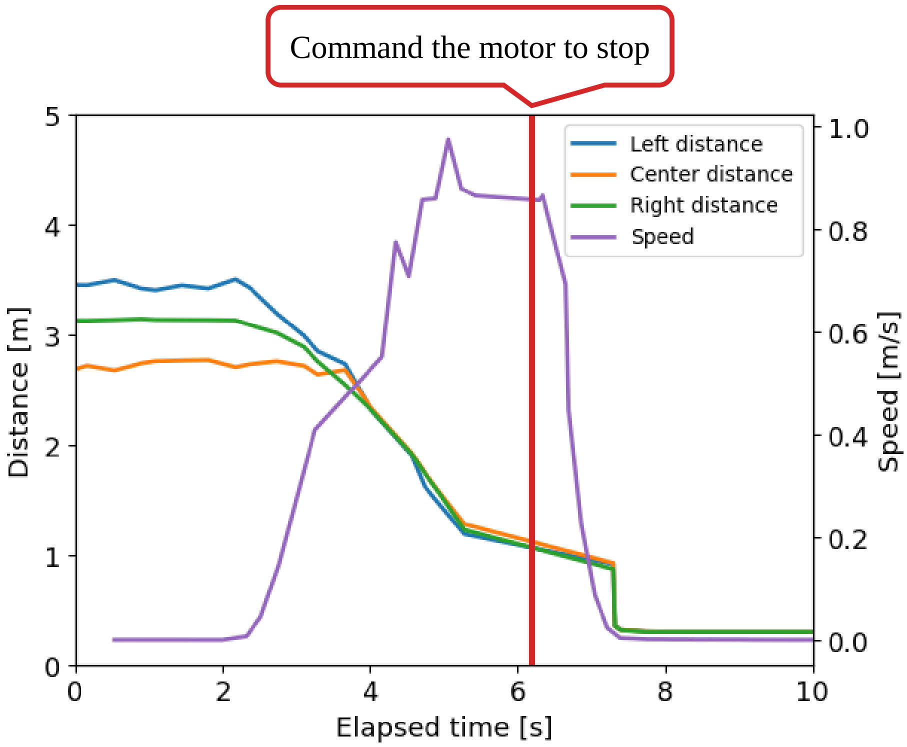

Figure 5.7: Relationship between depth image distance and velocity when walking straight ahead vertically to the wall.

front, left, and right 45-degree directions, the collision avoidance function successfully prevented collisions with both walls and obstacles.

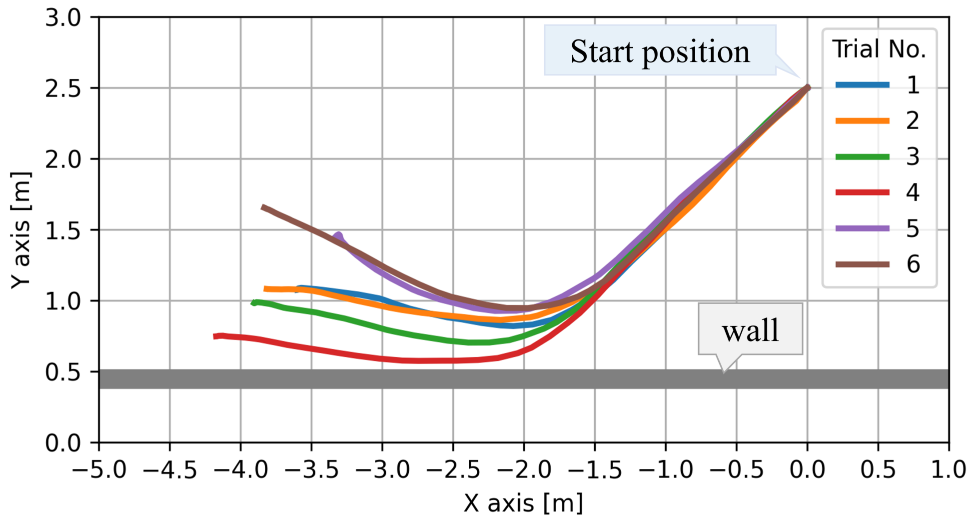

Figure 5.8: Overhead view of the trajectory for walker when moving straight ahead at 45 ° to the left relative to the wall.

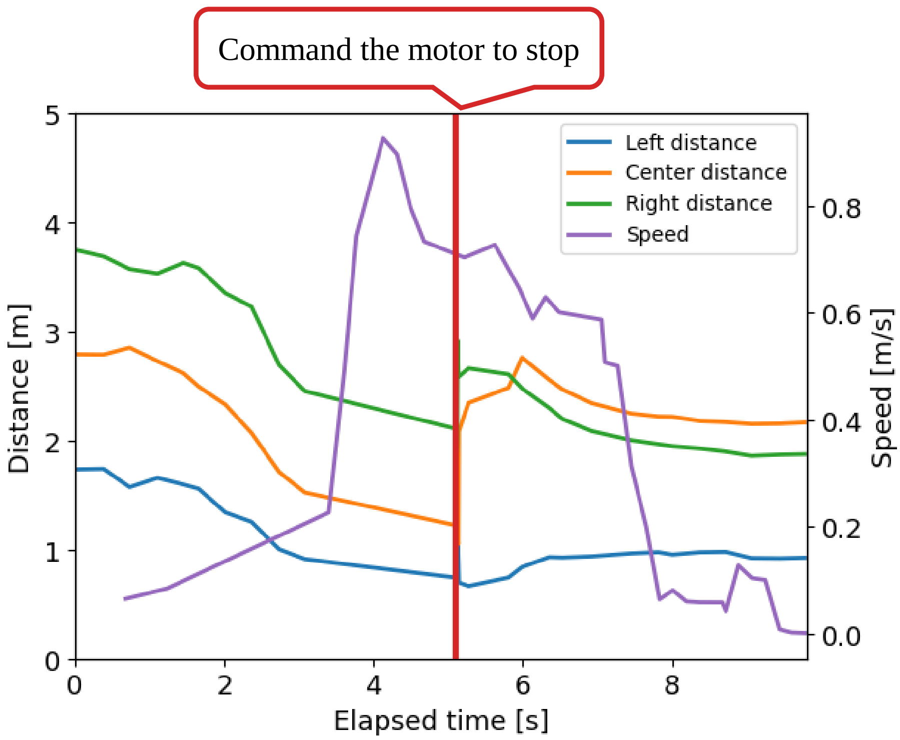

Figure 5.9: Relationship between depth image distance and velocity when walking straight ahead at 45 ° to the left relative to the wall.

Chapter 6

Conclusion

This study delved into the challenges faced by individuals who require mild walking assistance within care facilities using walkers. By proposing tailored solutions for each issue, a smart walker with an electrically assisted motor was developed to promote independent walking for those in need of care. The key points of this study are summarized below.

Chapter 1 provided an overview of the background and objectives of the study. With the aging population, improving the quality of life (QOL) of the elderly has garnered significant attention. Maintaining the independent living functions of the elderly is crucial, particularly the ability to walk independently in this social context, making walkers a vital assistive device. This study examined the use of walkers as assistive devices to promote independent walking. The challenges of utilizing walkers in nursing care facilities were analyzed, and three key issues were outlined in this study.

Chapter 2 explores the impact of walking on individuals, importance of walking support, and evolution of walking aids. By organizing existing knowledge, this chapter demonstrated the relevance of the study's issues and solutions within the context of conventional methods. It discussed the physical benefits of walking, need for walking support, and emphasized the significance of this study. This chapter outlined the key considerations for designing the proposed smart walker, which was the primary focus of this research. It discussed the challenges that needed to be addressed in the development of walking aids. The chapter also provided a summary of the approaches utilized in previous studies to address similar issues, regardless of the type of walking aid. Additionally, it described the unique features of the approach adopted in this research and argued for its validity.

Chapter 3 delved into the development of a smart walker system and the implementation of autonomous navigation functions to address the challenges identified in chapter 1. This chapter revealed that the accessibility of a walker may be limited in nursing care facilities, creating a burden for individuals who must retrieve a walker from a distant location. To mitigate these issues, a smart walker system with autonomous navigation capabilities was proposed. The autonomous navigation function, utilizing a stereo camera and ROS, has been successfully developed. The performance in reaching the target point was assessed by analyzing the results of self-position estimation. Additionally, the tracking accuracy of the target path was evaluated by measuring the cross-track error between the target and actual paths. The effectiveness of the autonomous navigation function in navigating the general path typically found in nursing homes was demonstrated through the results of the experiment.

Chapter 4 examined propulsion assistance functions in smart walkers, focusing on scenarios in which users may struggle to maintain a desired walking speed. A PID control was introduced to ensure safe walking within nursing care facilities. Evaluation experiments were conducted using a forearm-supported walker equipped with motor torque for propulsion assistance. Both subjective (questionnaire survey) and objective (surface electromyography) methods were employed to assess the system's impact on reducing walking load and lower limb muscle activity. The findings demonstrated that motor-assisted propulsion effectively reduced leg strain during short-term walking and altered lower limb muscle activity. Additionally, performance evaluations validated the system's reliable speed tracking and its compatibility with walking, as evidenced through simulated weight-based tests and trials with participants.

Chapter 5 details the findings of research conducted on collision avoidance utilizing depth images. Collisions and other incidents resulting in falls were identified as significant contributors to external injuries and the need for nursing care among walker users. To mitigate collisions while using a walker, the optimal collision avoidance direction and control intensity should be dynamically adjusted based on the situation of the forward environment and moving speed of the walker. This study introduced a collision avoidance feature that leveraged motor control, integrating depth images and walker speed data. In the experiment, obstacles, such as walls and beds were designated as targets for collision avoidance, and the accuracy of obstacle direction estimation and collision avoidance functionality was assessed. The experimental results demonstrated the effectiveness of the collision prevention feature in specific scenarios involving walls and obstacles, as evidenced by the observed changes in walker trajectory and speed changes when approaching from the front and 45 degrees to the left and right.

Based on the aforementioned findings, the development of a smart walker to address the three primary challenges associated with traditional walkers was discussed. While this study focused on the issues specific to walker usage, similar challenges exist with other mobility aids. Some of the proposed features could potentially be adapted for use in aids with comparable characteristics. Regrettably, the experiment conducted in this study was unable to validate the proposed system with real-world users, such as individuals who rely on walkers and residents of nursing care facilities. This primarily resulted from the fact that the proposed smart walker system did not satisfy the necessary safety standards for testing with individuals with unstable walking. Additionally, logistical challenges stemming from the COVID-19 pandemic hindered the ability to conduct on-site demonstrations at nursing care facilities. In the future, a demonstration experiment should be conducted for the assumed users in an experimental setting that minimizes the risk of falls, to assess the effectiveness of each proposed function.

This study has made a significant contribution by addressing the challenges associated with the use of walkers in nursing care facilities. A smart walker system with an electric assist function has been developed to effectively address these issues. Unlike other research on smart walkers that primarily focus on the needs of care recipients, this study stands out by considering designs that are user-friendly for caregivers and facilities as well. Furthermore, this study offers a solution to the growing problem of an increasing number of care recipients and a shortage of caregivers, which results from the aging population from the perspective of engineering and information science.

Acknowledgements

I would like to extend my sincerest gratitude to Professor Hidenori Kawamura for his invaluable guidance and support, which enabled me to thrive in my research endeavors.

I would also like to express my gratitude for the insightful comments provided by the professor. Furthermore, I would like to express my gratitude to Professors Itsuki Noda, Masahito Yamamoto, and Tetsuo Ono of Hokkaido University for their valuable feedback on this study. I am also thankful to Associate Professor Tomohisa Yamashita and Assistant Professor Soichiro Yokoyama for their insightful discussions and remarks. Additionally, I am grateful to Professor Norio Kato for providing valuable perspectives from a physical therapist's viewpoint and for his assistance with experimental measurements. I would like to acknowledge Masato Mori of SUNCREER Co., Ltd. for his invaluable feedback on the study subjects and system design. Without their enthusiastic support, this research would not have been possible.

I would also like to acknowledge the students of the Laboratory of Harmonious Systems Engineering for their valuable discussions and research contributions that have significantly helped in the completion of this study.

Finally, I would like to thank my family for their support, without whom I would not have been able to complete my research.

References

[1] James Lubitz, Liming Cai, Ellen Kramarow, and Harold Lentzner. Health, life expectancy, and health care spending among the elderly. *New England Journal of Medicine*, 349(11):1048–1055, 2003.

[2] Joshua A Salomon, Haidong Wang, Michael K Freeman, Theo Vos, Abraham D Flaxman, Alan D Lopez, and Christopher JL Murray. Healthy life expectancy for 187 countries, 1990–2010: a systematic analysis for the global burden disease study 2010. *The Lancet*, 380(9859):2144–2162, 2012.

[3] Marcia A Testa and Donald C Simonson. Assessment of quality-of-life outcomes. *New England journal of medicine*, 334(13):835–840, 1996.

[4] Chosa Etsuo. Locomotive syndrome, musculoskeletal ambulation disorder symptom complex, frailty and sarcopenia : Prevention and rehabilitation. *The Japanese Journal of Rehabilitation Medicine*, 50(1):48–54, 2013.

[5] Labour Ministry of Health and Welfare. Long-term care-needs certification (in japanese). `https://www.mhlw.go.jp/topics/kaigo/nintei/gaiyo1.html`. Accessed on November 1, 2024.

[6] Jack M Guralnik, Laurence G Branch, Steven R Cummings, and J. David Curb. Physical Performance Measures in Aging Research. *Journal of Gerontology*, 44(5):M141–M146, 1989.

[7] Robert D Abbott, Lon R White, G Webster Ross, Kamal H Masaki, J. David Curb, and Helen Petrovitch. Walking and Dementia in Physically Capable Elderly Men. *JAMA*, 292(12):1447–1453, 2004.

[8] Jamie S McPhee, David P French, Dean Jackson, James Nazroo, Neil Pendleton, and Hans Degens. Physical activity in older age: perspectives for healthy ageing and frailty. *Biogerontology*, 17(3):567–580, 2016.

[9] Colleen G Canning, Louise Ada, Justin J Johnson, and Stephanie McWhirter. Walking capacity in mild to moderate parkinson's disease. *Archives of Physical Medicine and Rehabilitation*, 87(3):371–375, 2006.

[10] Labour Ministry of Health and Welfare. Summary report of comprehensive survey of living conditions 2016 (in japanese). `https://www.mhlw.go.jp/toukei/saikin/hw/k-tyosa/k-tyosa16/`. Accessed on June 20, 2024.

[11] Yumiko Arai and Steven H Zarit. Exploring strategies to alleviate caregiver burden: Effects of the national long-term care insurance scheme in japan. *Psychogeriatrics*, 11(3):183–189, 2011.

[12] Jehangir Arshad, Muhammad Adil Ashraf, Hafiza Mahnoor Asim, Nouman Rasool, Mujtaba Hussain Jaffery, and Shahid Iqbal Bhatti. Multi-mode electric wheelchair with health monitoring and posture detection using machine learning techniques. *Electronics*, 12(5), 2023.

[13] Pei Di, Yasuhisa Hasegawa, Shotaro Nakagawa, Kosuke Sekiyama, Toshio Fukuda, Jian Huang, and Qiang Huang. Fall detection and prevention control using walking-aid cane robot. *IEEE/ASME Transactions on Mechatronics*, 21(2):625–637, 2016.

[14] Hui-Ya Chen, Hsiu-I Chen, Shu-Yi Fu, Chun-Hou Wang, and Ya-Wen Hsieh. Attentional demands of cane-free walking and cane walking in subacute stroke patients who have just learned to walk without a cane. *International journal of rehabilitation research*, 44(4):377–381, 2021.

[15] Kap-Ho Seo and Ju-Jang Lee. The development of two mobile gait rehabilitation systems. *IEEE transactions on neural systems and rehabilitation engineering*, 17(2):156–166, 2009.

[16] Kimberly Nickerson, Kailey Diaz, and Brittney Muir. Circumstances of falls among older adult walker users in long-term care and the associated walker design deficits. *Assistive Technology*, 36(3):248–253, 2023.

[17] Shane MacNamara and Gerard Lacey. A smart walker for the frail visually impaired. In *Proceedings 2000 ICRA. Millennium Conference. IEEE International Conference on Robotics and Automation. Symposia Proceedings (Cat. No. 00CH37065)*, volume 2, pages 1354–1359, 2000.

[18] Gerard Lacey and Shane MacNamara. Context-aware shared control of a robot mobility aid for the elderly blind. *The International Journal of Robotics Research*, 19(11):1054–1065, 2000.

[19] Yuto Mori, Soichiro Yokoyama, Tomohisa Yamashita, Hidenori Kawamura, and Masato Mori. Development of a forearm-supported walker with walking support and autonomous driving functions. In *26th International Symposium on Artificial Life and Robotics (AROB 26th 2021)*, pages 170–175, 2021.

[20] Yuto Mori, Soichiro Yokoyama, Tomohisa Yamashita, Hidenori Kawamura, Norio Kato, and Masato Mori. Development of an autonomous forearm-supported walker for nursing facilities. *Artificial Life and Robotics*, 26:432–441, 2021.

[21] Yuto Mori, Soichiro Yokoyama, Tomohisa Yamashita, Hidenori Kawamura, and Masato Mori. Development of assistance level adjustment function for variable load on a forearm-supported robotic walker. *Sensors*, 24(19):6456, 2024.

[22] Yuto Mori, Soichiro Yokoyama, Tomohisa Yamashita, Hidenori Kawamura, and Masato Mori. Obstacle avoidance using depth imaging for forearm-supported four-wheeled walker with walking assist. In *2023 20th International Conference on Ubiquitous Robots (UR)*, pages 544–551, 2023.

[23] Robert J Jaeger, Gary M Yarkony, and Elliot J Roth. Rehabilitation technology for standing and walking after spinal cord injury. *American journal of physical medicine & rehabilitation*, 68(3):128–133, 1989.

[24] Roma Robertson, Ann Robertson, Ruth Jepson, and Margaret Maxwell. Walking for depression or depressive symptoms: a systematic review and meta-analysis. *Mental health and physical activity*, 5(1):66–75, 2012.

[25] Ling-Ling Lee, Michael C Watson, Caroline A Mulvaney, Chin-Chueh Tsai, and Shu-Fen Lo. The effect of walking intervention on blood pressure control: a

systematic review. *International journal of nursing studies*, 47(12):1545–1561, 2010.

[26] Martin Wohlrab, Jochen Klenk, Laura Delgado-Ortiz, Michael Chambers, Lynn Rochester, Matthias Zuchowski, Matthias Schwab, Clemens Becker, and Simon U Jaeger. The value of walking: a systematic review on mobility and healthcare costs. *European Review of Aging and Physical Activity*, 19(1: 31), Dec 2022.

[27] Tomoo Marukawa. The demand for and supply of elderly care in japan. *The Japanese Political Economy*, 48(1):8–26, 2022.

[28] Ayumi Honda, Yutaka Date, Yasuyo Abe, Kiyoshi Aoyagi, and Sumihisa Honda. Work-related stress, caregiver role, and depressive symptoms among japanese workers. *Safety and Health at Work*, 5(1):7–12, 2014.

[29] Satoshi Hayashi, Seishi Terada, Shigeto Nagao, Chikako Ikeda, Aki Shindo, Etsuko Oshima, Osamu Yokota, and Yosuke Uchitomi. Burden of caregivers for patients with mild cognitive impairment in japan. *International Psychogeriatrics*, 25(8):1357–1363, 2013.

[30] Jian Huang, Pei Di, Kouhei Wakita, Toshio Fukuda, and Kosuke Sekiyama. Study of fall detection using intelligent cane based on sensor fusion. In *2008 International Symposium on Micro-NanoMechatronics and Human Science*, pages 495–500, 2008.

[31] Kohei Wakita, Jian Huang, Kosuke Sekiyama, and Toshio Fukuda. Real-time fall detection and prevention control using intelligent cane for human operator. In *The Abstracts of the international conference on advanced mechatronics: toward evolutionary fusion of IT and mechatronics: ICAM 2010.5*, pages 265–270. The Japan Society of Mechanical Engineers, 2010.

[32] Dennis R Louie and Janice J Eng. Powered robotic exoskeletons in post-stroke rehabilitation of gait: a scoping review. *Journal of neuroengineering and rehabilitation*, 13:1–10, 2016.

[33] Bing Chen, Chun-Hao Zhong, Xuan Zhao, Hao Ma, Xiao Guan, Xi Li, Feng-Yan Liang, Jack Chun Yiu Cheng, Ling Qin, Sheung-Wai Law, and Wei-Hsin Liao.

A wearable exoskeleton suit for motion assistance to paralysed patients. *Journal of Orthopaedic Translation*, 11:7–18, 2017.

[34] Julie Vaughan-Graham, Dina Brooks, Lowell Rose, Goldie Nejat, Jose Pons, and Kara Patterson. Exoskeleton use in post-stroke gait rehabilitation: A qualitative study of the perspectives of persons post-stroke and physiotherapists. *Journal of neuroengineering and rehabilitation*, 17:1–15, 2020.

[35] Helene Brännström, Margit Bäckman, and Regina Santamäki Fischer. Walking on the edge: meanings of living in an ageing body and using a walker in everyday life–a phenomenological hermeneutic study. *International Journal of Older People Nursing*, 8(2):116–122, 2013.

[36] William C Mann, Dianne Hurren, and Machiko Tomita. Comparison of assistive device use and needs of home-based older persons with different impairments. *The American Journal of Occupational Therapy*, 47(11):980–987, 1993.

[37] Laura N Gitlin and Desirée Burgh. Issuing assistive devices to older patients in rehabilitation: An exploratory study. *The American Journal of Occupational Therapy*, 49(10):994–1000, 1995.

[38] Ken Pippin and Geoffrey R Femie. Designing devices that are acceptable to the frail elderly: a new understanding based upon how older people perceive a walker. *Technology and Disability*, 7:93–102, 1997.

[39] Daisuke Fujita, Kenichi Kobara, Hiroshi Osaka, Susumu Watanabe, Teppei Sintani, Takuya Sugimura, Kenji Makino, Tim Cleminson, and Tunayoshi Morikawa. The influence of rollators with forearm support on walking speed, endurance and dynamic balance. *Journal of Physical Therapy Science*, 24(8):667–670, 2012.

[40] Luca Cavanini, Gionata Cimini, Francesco Ferracuti, Alessandro Freddi, Gianluca Ippoliti, Andrea Monteriù, and Federica Verdini. A qr-code localization system for mobile robots: application to smart wheelchairs. In *2017 European conference on mobile robots (ECMR)*, pages 1–6. IEEE, 2017.

[41] Cimini Gionata, Ferracuti Francesco, Freddi Alessandro, Iarlori Sabrina, and Monteriu Andrea. An inertial and qr code landmarks-based navigation system

for impaired wheelchair users. In *Ambient Assisted Living: Italian Forum 2013*, pages 205–214, 2014.

[42] Loiy Habha, Urvish Trivedi, Redwan Alqasemi, and Rajiv Dubey. Autonomous wheelchair indoor-outdoor navigation system through accessible routes. In *Proceedings of the 14th PErvasive Technologies Related to Assistive Environments Conference*, pages 199–202, 2021.

[43] Abhayjeet Juneja, Lakshay Bhandari, Hamed Mohammadbagherpoor, Anand Singh, and Edward Grant. A comparative study of slam algorithms for indoor navigation of autonomous wheelchairs. In *2019 IEEE International Conference on Cyborg and Bionic Systems (CBS)*, pages 261–266, 2019.

[44] Korbinian Schmid, Teodor Tomic, Felix Ruess, Heiko Hirschmüller, and Michael Suppa. Stereo vision based indoor/outdoor navigation for flying robots. In *2013 IEEE/RSJ international conference on intelligent robots and systems*, pages 3955–3962, 2013.

[45] Xiaolong Hui, Jiang Bian, Xiaoguang Zhao, and Min Tan. Vision-based autonomous navigation approach for unmanned aerial vehicle transmission-line inspection. *International Journal of Advanced Robotic Systems*, 15(1):1729881417752821, 2018.

[46] Boyu Gao, Haoxiang Lang, and Jing Ren. Stereo visual slam for autonomous vehicles: A review. In *2020 IEEE International Conference on Systems, Man, and Cybernetics (SMC)*, pages 1316–1322, 2020.

[47] Sherif AS Mohamed, Mohammad-Hashem Haghbayan, Tomi Westerlund, Jukka Heikkonen, Hannu Tenhunen, and Juha Plosila. A survey on odometry for autonomous navigation systems. *IEEE access*, 7:97466–97486, 2019.

[48] Teddy Ort, Liam Paull, and Daniela Rus. Autonomous vehicle navigation in rural environments without detailed prior maps. In *2018 IEEE international conference on robotics and automation (ICRA)*, pages 2040–2047. IEEE, 2018.

[49] Annett Chilian and Heiko Hirschmüller. Stereo camera based navigation of mobile robots on rough terrain. In *2009 IEEE/RSJ International Conference on Intelligent Robots and Systems*, pages 4571–4576, 2009.

[50] Kaivuan Gao, Jing Xin, Han Cheng, Ding Liu, and Jiang Li. Multi-mobile robot autonomous navigation system for intelligent logistics. In *2018 Chinese Automation Congress (CAC)*, pages 2603–2609, 2018.

[51] Spyros G Tzafestas. Mobile robot control and navigation: A global overview. *Journal of Intelligent & Robotic Systems*, 91:35–58, 2018.

[52] Maria M Martins, Anselmo Frizera-Neto, Cristina P Santos, and Ramón Ceres Ruíz. Smart walker control through the inference of the user's command intentions. In *Proceedings of the 9th International Conference on Informatics in Control, Automation and Robotics*, volume 1, pages 458–463, 2012.

[53] Maria Martins, Cristina Santos, Eurico Seabra, Luis Basílio, and Anselmo Frizera. A new integrated device to read user intentions when walking with a smart walker. In *2013 11th IEEE International Conference on Industrial Informatics (INDIN)*, pages 299–304, 2013.

[54] Joao Paulo, Paulo Peixoto, and Urbano J Nunes. Isr-aiwalker: Robotic walker for intuitive and safe mobility assistance and gait analysis. *IEEE Transactions on Human-Machine Systems*, 47(6):1110–1122, 2017.

[55] Geunho Lee, Takanori Ohnuma, and Nak Young Chong. Design and control of jaist active robotic walker. *Intelligent Service Robotics*, 3(3):125–135, 2010.

[56] Geunho Lee, Eui-Jung Jung, Takanori Ohnuma, Nak Young Chong, and Byung-Ju Yi. Jaist robotic walker control based on a two-layered kalman filter. In *2011 IEEE international conference on robotics and automation*, pages 3682–3687, 2011.

[57] Simone T Boerema, Lex van Velsen, Miriam MR Vollenbroek-Hutten, and Hermie J Hermens. Value-based design for the elderly: An application in the field of mobility aids. *Assistive Technology*, 29(2):76–84, 2017.

[58] Vianda S Stel, Johannes H Smit, Saskia MF Pluijm, and Paul Lips. Consequences of falling in older men and women and risk factors for health service use and functional decline. *Age and ageing*, 33(1):58–65, 2004.

[59] Nancy M Gell, Robert B Wallace, Andrea Z LaCroix, Tracy M Mroz, and Kushang V Patel. Mobility device use in older adults and incidence of falls

and worry about falling: Findings from the 2011–2012 national health and aging trends study. *Journal of the American Geriatrics Society*, 63(5):853–859, 2015.

[60] Christopher Feltner, Jonathan Guilbe, Sharare Zehtabian, Siavash Khodadadeh, Ladislau Boloni, and Damla Turgut. Smart walker for the visually impaired. In *ICC 2019-2019 IEEE international conference on communications (ICC)*, pages 1–6, 2019.

[61] Andrew J Rentschler, Richard Simpson, Rory A Cooper, and Michael L Boninger. Clinical evaluation of guido robotic walker. *Journal of Rehabilitation Research & Development*, 45(9), 2008.

[62] StereoLabs. Zed 2 - ai stereo camera. `https://www.stereolabs.com/en-jp/products/zed-2`. Accessed on November 10, 2024.

[63] NVIDIA. Jetson nano brings the power of modern ai to edge devices. `https://www.nvidia.com/en-us/autonomous-machines/embedded-systems/jetson-nano`. Accessed on November 10, 2024.

[64] Arduino. Uno r3 — arduino documentation. `https://docs.arduino.cc/hardware/uno-rev3/`. Accessed on November 10, 2024.

[65] Mathieu Labbé and François Michaud. Online global loop closure detection for large-scale multi-session graph-based slam. In *2014 IEEE/RSJ International Conference on Intelligent Robots and Systems*, pages 2661–2666. IEEE, 2014.

[66] Mathieu Labbé and François Michaud. Long-term online multi-session graph-based splam with memory management. *Autonomous Robots*, 42:1133–1150, 2018.

[67] Mathieu Labbé and François Michaud. Rtab-map as an open-source lidar and visual simultaneous localization and mapping library for large-scale and long-term online operation. *Journal of field robotics*, 36(2):416–446, 2019.

[68] Yun Li, Kiam Heong Ang, and Gregory CY Chong. Pid control system analysis and design. *IEEE Control Systems Magazine*, 26(1):32–41, 2006.

[69] Ning Zhang, Francesco Nex, George Vosselman, and Norman Kerle. Lite-mono: A lightweight cnn and transformer architecture for self-supervised monocular

depth estimation. In *Proceedings of the IEEE/CVF Conference on Computer Vision and Pattern Recognition*, pages 18537–18546, 2023.

[70] Clément Godard, Oisin Mac Aodha, Michael Firman, and Gabriel J Brostow. Digging into self-supervised monocular depth estimation. In *Proceedings of the IEEE/CVF international conference on computer vision*, pages 3828–3838, 2019.

[71] Jiwon Shin, Andrey Rusakov, and Bertrand Meyer. Smartwalker: An intelligent robotic walker. *Journal of Ambient Intelligence and Smart Environments*, 8(4):383–398, 2016.

[72] Kiwan Han, Byung-Woo Ko, Joon-Ho Shin, Woonghee Cho, and Won-Kyung Song. Usability testing of smart mobile walker: A pilot study. In *2014 11th International Conference on Ubiquitous Robots and Ambient Intelligence (URAI)*, pages 112–115, 2014.

[73] Kenneth G Holt, Suh Fang Jeng, Robert Ratcliffe, and Joseph Hamill. Energetic cost and stability during human walking at the preferred stride frequency. *Journal of motor behavior*, 27(2):164–178, 1995.

[74] Hao Howe Liu, Margaret McGee, Wen Wang, and Mary Persson. Comparison of gait characteristics between older rolling walker users and older potential walker users. *Archives of Gerontology and Geriatrics*, 48(3):276–280, 2009.

[75] Jeffrey R Cram. The history of surface electromyography. *Appl Psychophysiol Biofeedback*, 28(2):81–91, 2003.

[76] Catherine Disselhorst-Klug, Thomas Schmitz-Rode, and Günter Rau. Surface electromyography and muscle force: Limits in semg–force relationship and new approaches for applications. *Clinical Biomechanics*, 24(3):225–235, 2009.

[77] Min-Chi Chiu, Hsin-Chieh Wu, and Li-Yu Chang. Gait speed and gender effects on center of pressure progression during normal walking. *Gait & posture*, 37(1):43–48, 2013.

[78] Ruijie Quan, Linchao Zhu, Yu Wu, and Yi Yang. Holistic lstm for pedestrian trajectory prediction. *IEEE transactions on image processing*, 30:3229–3239, 2021.

[79] Hongyan Guo, Chen Shen, Hui Zhang, Hong Chen, and Rui Jia. Simultaneous trajectory planning and tracking using an mpc method for cyber-physical systems: A case study of obstacle avoidance for an intelligent vehicle. *IEEE Transactions on Industrial Informatics*, 14(9):4273–4283, 2018.

[80] Sergio D Sierra M, Mario Garzón, Marcela Múnera, and Carlos A Cifuentes. Human–robot–environment interaction interface for smart walker assisted gait: Agora walker. *Sensors*, 19(13):2897, 2019.